

CERN-EP-2017-090
2021/10/20

CMS-B2G-16-016

Searches for W' bosons decaying to a top quark and a bottom quark in proton-proton collisions at 13 TeV

The CMS Collaboration*

Abstract

Searches are presented for heavy gauge bosons decaying into a top and a bottom quark in data collected by the CMS experiment at $\sqrt{s} = 13$ TeV that correspond to an integrated luminosity of 2.2 and 2.6 fb⁻¹ in the leptonic and hadronic analyses, respectively. Two final states are analyzed, one containing a single electron, or muon, and missing transverse momentum, and the other containing multiple jets and no electrons or muons. No evidence is found for a right-handed W' boson (W'_R) and the combined analyses exclude at 95% confidence level W'_R with masses below 2.4 TeV if $M_{W'_R} \gg M_{\nu_R}$ (mass of the right handed neutrino), and below 2.6 TeV if $M_{W'_R} < M_{\nu_R}$. The results provide the most stringent limits for right-handed W' bosons in the top and bottom quark decay channel.

Published in the Journal of High Energy Physics as doi:10.1007/JHEP08(2017)029.

arXiv:1706.04260v2 [hep-ex] 10 Aug 2017

1 Introduction

Many theories that extend the standard model (SM) predict additional charged gauge bosons [1–5], often referred to as W' bosons. In models where the resonance is sufficiently massive, it is common to postulate that the coupling to third generation quarks might be enhanced relative to the second and first generations [6, 7], making a search for the decay $W' \rightarrow t\bar{b}$ or $\bar{t}b$ highly appropriate. A particular advantage of this kind of search is that this channel is more easily distinguished from the large continuum of multijet background than searches in the decays to light quarks ($W' \rightarrow q\bar{q}$). The search in top and bottom quark (tb) systems complements searches in $W' \rightarrow \ell\nu$ (where ℓ denotes a charged lepton and ν denotes a neutrino) and $W' \rightarrow VV$ (where V denotes an SM W or Z boson) channels. The tb final state also benefits from the fact that its W' mass can be fully determined, whereas in the leptonic mode there is a two-fold ambiguity in its mass.

This paper presents the first search performed for a right-handed W' (W'_R) decaying to a top and a bottom quark at $\sqrt{s} = 13$ TeV, using data collected by the CMS experiment corresponding to an integrated luminosity of up to 2.6 fb^{-1} . In scenarios where a theoretical right-handed neutrino (ν_R) is heavier than the W'_R , the decay $W'_R \rightarrow \ell\nu_R$ is forbidden and the branching fraction $\mathcal{B}(W'_R \rightarrow t\bar{b})$ is enhanced. This makes the $W'_R \rightarrow t\bar{b}$ decay an important channel in the search for W' bosons. Previous searches in the tb channel have been performed at the Fermilab Tevatron [8–10] and at the CERN LHC by both the CMS [11, 12] and ATLAS [13, 14] Collaborations. The most stringent limits to date on the production of W' bosons with purely right-handed couplings come from the CMS search performed at $\sqrt{s} = 8$ TeV [12]. Relative to this 8 TeV search, the expected production cross section of the W'_R boson at $\sqrt{s} = 13$ TeV is enhanced by a factor of approximately 7 (13) for a 2 (3) TeV resonance.

We separately analyze events with and without a lepton in the final state (referred to as leptonic and hadronic analyses), and then combine the results. In both analyses, the invariant mass of the tb system ($M_{t\bar{b}}$) is used to conduct searches for the W'_R boson. The achieved sensitivity after combining the results is better than in each individual channel, thereby providing improved exclusion limits compared to previous results.

In this paper, Section 2 contains a description of the CMS detector. Section 3 provides details of the simulated samples and their production, while Section 4 discusses the techniques used for object reconstruction and event selection. The methods used for estimation of backgrounds are given in Section 5. Section 6 provides information on systematic uncertainties, and Section 7 presents results of the individual and combined analyses. A summary is given in Section 8.

2 The CMS detector

The central feature of the CMS apparatus is a superconducting solenoid of 6 m internal diameter, providing a magnetic field of 3.8 T. A silicon pixel and strip tracker, a lead tungstate crystal electromagnetic calorimeter (ECAL), and a brass and scintillator hadron calorimeter (HCAL), each composed of a barrel and two endcap sections, reside within the solenoid field. Forward calorimeters extend the pseudorapidity (η) coverage [15] provided by the barrel and endcap detectors. Muons are measured in gas-ionization detectors embedded in the steel flux-return yoke outside the solenoid.

The electron momentum is estimated by combining the energy measurement in the ECAL with the momentum measurement in the tracker. The momentum resolution for electrons with $p_T \approx 45$ GeV from $Z \rightarrow e^+e^-$ decays ranges from 1.7% for electrons without an accompanying

shower in the barrel region, to 4.5% for electrons showering in the endcaps [16].

Muons are measured in the range $|\eta| < 2.4$, with detection planes based on drift tubes, cathode strip chambers, and resistive plate chambers. Matching muons to tracks in the silicon tracker yields a relative p_T resolution for muons with $20 < p_T < 100$ GeV of 1.3–2.0% in the barrel and better than 6% in the endcaps. The p_T resolution in the barrel is better than 10% for muons with p_T up to 1 TeV [17].

Events of interest are selected using a two-tiered trigger system [18]. The first level (L1), composed of custom hardware processors, uses information from the calorimeters and muon detectors to select events at a rate of around 100 kHz within a time interval of less than 4 μ s. The second level, known as the high-level trigger (HLT), consists of a farm of processors running a version of the full event reconstruction software optimized for fast processing, and reduces the event rate to less than 1 kHz before data storage.

The particle-flow event algorithm [19–21] reconstructs and identifies each individual particle candidate using an optimized combination of information from the various elements of the CMS detector. The energy of photons is obtained from the ECAL measurement, and corrected for the online suppression of signals close to threshold. The energy of electrons is determined from a combination of the electron momentum at the primary interaction vertex determined by the tracker, the energy of the corresponding ECAL cluster, and the energy sum of all bremsstrahlung photons spatially compatible with originating from the electron track. The energy of muons is obtained from the curvature of the corresponding track. The energy of charged hadrons is determined from a combination of their momentum measured in the tracker and the matching ECAL and HCAL energy deposition, corrected for suppression of small signals and for the response of hadron showers in the calorimeters. Finally, the energy of neutral hadrons is obtained from the corresponding corrected ECAL and HCAL energies.

The missing transverse momentum vector, \vec{p}_T^{miss} , is defined as the projection on the plane perpendicular to the beams of the negative vector sum of the momenta of all reconstructed particles in an event.

A more detailed description of the CMS detector, together with a definition of the coordinate system and the kinematic variables, can be found in Ref. [15].

3 Modeling of signal and background

All signal events are generated at leading order (LO) using the CompHEP 4.5.2 [22] package and their cross sections are scaled to next-to-leading order (NLO) with an approximate K-factor of 1.2 [23, 24]. All signal samples are generated with purely right-handed couplings, according to the following model-independent, lowest-order, effective Lagrangian:

$$\mathcal{L} = \frac{V_{f_i f_j}}{2\sqrt{2}} g_W \bar{f}_i \gamma_\mu (1 + \gamma^5) W'^\mu f_j + \text{H.C.}, \quad (1)$$

where $V_{f_i f_j}$ is the element of the Cabibbo–Kobayashi–Maskawa matrix when f is a quark, and $V_{f_i f_j} = \delta_{ij}$ when f is a lepton, and g_W is the SM weak coupling constant. Since we consider W'_R bosons (with right-handed couplings), there is no interference at production with the SM W boson. The simulation for leptonic decays of the W'_R boson includes decays involving a τ lepton, and no distinction is made in the analysis between an electron or muon directly from the W boson decay and an electron or muon from a subsequent leptonic τ decay. Signal samples are generated for signal masses between 1 and 3 TeV in 100 GeV steps. The width of the W'_R

generated by COMPHEP is narrow, and varies with the mass, but is approximately 3% for all masses considered in this analysis. This is smaller than the invariant mass resolution of the detector, and therefore the precise values of the width does not have a significant effect on our results.

For right-handed W' bosons, the leptonic decays necessarily produce right-handed neutrinos (ν_R). When the mass of the ν_R is larger than that of the W'_R boson ($M_{W'_R} < M_{\nu_R}$) then the $W'_R \rightarrow \ell \nu_R$ decays are kinematically forbidden and only $W'_R \rightarrow q\bar{q}'$ decays are allowed (of which $W'_R \rightarrow t\bar{b}$ is a subset). On the other hand, if the ν_R is lighter than the W'_R boson ($M_{W'_R} > M_{\nu_R}$) then $W'_R \rightarrow \ell \nu_R$ decays are allowed. Consequently, the product of the W'_R cross section and its branching fraction ($W' \rightarrow t\bar{b}$) is enhanced for heavy neutrinos by approximately one third. When calculating the distribution in the number of expected signal events, it is always assumed that $M_{W'_R} \gg M_{\nu_R}$. When displaying upper limits at 95% confidence levels (CL), we consider both scenarios.

The SM processes that contribute significantly to the background in the leptonic analysis are W +jets and $t\bar{t}$ events. The background in the hadronic analysis is dominated by multijet and $t\bar{t}$ production. Although it is a much smaller contribution to the total background, both analyses also consider associated production of a top quark and a W boson as background, while the leptonic analysis further considers both t - and s -channel single top quark, Z or γ^* +jets, and diboson (WW , WZ and ZZ) production. The hadronic and leptonic analyses employ different methods of background estimation because of differences in the final states. All background predictions from nondominant sources are estimated from simulation.

Simulated samples for Z/γ^* +jets, s -, and t -channel single top, and W +jets are generated at NLO using the MADGRAPH5_aMC@NLO [25–27] v2.2.2 generator. The $t\bar{t}$ and single top quark in the tW channel samples are generated using the POWHEG v2 generator [28–32], and all other backgrounds are generated at LO using the PYTHIA 8.2 [33] generator. In all cases, NNPDF 3.0 parton distribution functions (PDFs) are used [34].

Both hadronic and leptonic analyses use the MC simulated $t\bar{t}$ background prediction. In the leptonic analysis, the $t\bar{t}$ simulation is assigned a correction based on the top quark p_T , which is known to be improperly modeled [35]. This correction is not necessary in the hadronic analysis because of differences in the phase space resulting from the specific event selections, and is confirmed in a $t\bar{t}$ enriched control region. The predictions from both analyses are checked in control regions that are independent with respect to the signal region and contain minimal contamination from signal. In both cases, the agreement between the data and prediction from simulation is good.

For the W +jets background in the leptonic analysis, the initial prediction is estimated from simulation. The agreement with data is then checked in a control region dominated by W +jets events. The same region is also used to extract correction factors for different W +jets components, e.g., W +light-quark or gluon jets and W +charm or bottom quark jets. The relative composition of these components in simulation is known to differ [36] from the composition in data, and we apply these correction factors to the predictions.

The multijet background in the hadronic analysis is determined from data in independent control regions. The validity of the estimation procedure is then checked using simulated multijet events.

More details on the background estimation methods can be found in Section 5.

All simulated signal and background events are processed through PYTHIA 8.2 for parton frag-

mentation and hadronization, where the underlying event tune CUETP8M1 [37] has been used. The simulation of the CMS detector is performed using GEANT4 [38]. Also, all simulated event samples include additional overlapping proton-proton interactions in the same or adjacent bunch crossings (pileup) that are weighted such that the distribution in the number of interactions agrees with that expected in data.

4 Event reconstruction and selection

The two analyses employ different selections targeted at their respective signal topologies. Details on specific aspects of the selections are given below.

4.1 Jet reconstruction

Jets are reconstructed offline from the particle-flow candidates, clustered using the anti- k_T algorithm [39, 40] with distance parameters of 0.4 (AK4 jets) and 0.8 (AK8 jets).

The jet momentum is defined by the vectorial sum of all particle-flow candidate momenta in the jet, and is found from simulation to be within 5 to 10% of the true momentum. An offset correction is applied to jet momenta to take into account the contribution from pileup. Jet energy corrections [41] are obtained from simulation, and are confirmed with in situ measurements of the energy balance in dijet and photon+jet events. Additional selection criteria are applied to each event to remove spurious jet-like features originating from isolated noise patterns in certain HCAL regions.

Both the leptonic and hadronic analyses use the charged-hadron subtraction method, which removes from the event any charged hadrons not associated with the leading vertex, defined as the vertex with the highest p_T^2 sum. The estimated contribution from pileup to the neutral hadron component of jets is also subtracted, based on the jet area [42].

The leptonic analysis uses AK4 jets because their smaller area makes them less sensitive to pileup, and the hadronic analysis uses AK8 jets whose larger area makes them more suited to the jet substructure-based techniques used to identify highly Lorentz-boosted top quark decays. These techniques are discussed in Section 4.1.2.

4.1.1 Identification of b jets

The combined secondary vertex version 2 (CSVv2) algorithm [43, 44], which combines secondary vertex and track based lifetime information in order to identify b jets, is used by both analyses. They use an operating point which has a b jet identification (b tagging) efficiency of 80% and a light-flavor jet misidentification (mistag) probability of 10%. A scale factor is applied as a function of p_T to correct observed differences in performance between data and simulation. In the hadronic analysis, an additional uncertainty is used to account for small differences in b tagging which arise from the larger jet-cone size. Details on the systematic uncertainty in b tagging can be found in Section 6.

4.1.2 Tagging of top quarks

The large Lorentz boost of the top quark from heavy W'_R boson ($M_{W'_R} \gtrsim 1$ TeV) decays causes the three jets from hadronic decays to merge into a single large-radius jet with distinct substructure. Variables that are sensitive to characteristics of this substructure can be used to discriminate signal from background. The hadronic analysis uses a top tagging algorithm that is based on three such variables: jet mass, N-subjettiness [45, 46], and subjet b tagging.

The jet mass is calculated after applying the modified mass-drop tagger, also known as the “soft drop” algorithm [47, 48], which reclusters the AK8 jet with the Cambridge–Aachen algorithm [49] and declusters until the following requirement is met:

$$\frac{\min(p_{T_1}, p_{T_2})}{p_{T_1} + p_{T_2}} > z(\Delta R_{12}/R_0)^\beta, \quad (2)$$

where p_{T_i} are the magnitude of the transverse momenta of the two subjet candidates, ΔR_{12} is the distance ($\Delta R = \sqrt{(\Delta\eta)^2 + (\Delta\phi)^2}$, where ϕ is the azimuthal angle in radians) between candidates, and R_0 is the jet size parameter. For this analysis, we use $z = 0.1$ and $\beta = 0$, and require the mass of the soft-drop declustered jet to be between 110 and 210 GeV, i.e. consistent with the top quark mass, M_{top} . For this operating point, the soft drop algorithm is equivalent to the modified mass-drop tagger [47, 50].

The N-subjettiness algorithm defines a series of τ_N variables that describe the consistency between the jet energy and the number of assumed subjets (N):

$$\tau_N = \frac{1}{d} \sum_i p_{T_i} \min(\Delta R_{1,i}, \Delta R_{2,i}, \dots, \Delta R_{N,i}), \quad (3)$$

where $\Delta R_{J,i}$ is the distance between the axis of the subjet candidate (J) and a specific constituent particle (i), and d is the normalization factor,

$$d = \sum_i p_{T_i} R, \quad (4)$$

where R is the distance parameter used in the jet clustering algorithm. The axes of the subjet candidate used to calculate N-subjettiness are found using the exclusive k_T algorithm [51], after which an optimization procedure is applied to minimize the N-subjettiness value, calculated using all particle-flow constituents of the AK8 jet. A jet with a low τ_N value will have energy deposited close to the axes of the N subjet candidates, which is a characteristic of a jet containing N subjets. A top quark jet is likely to be more consistent with three subjets than two, while a jet from a gluon or light quark will typically be consistent with either two or three subjets. Therefore, the ratio of τ_3 and τ_2 is characteristically smaller for top quark jets than for the multijet background. We select jets with $\tau_3/\tau_2 < 0.61$.

Finally, we apply the CSVv2 b tagging algorithm to the two soft-drop subjets of the candidate jet, and require the maximum b tagging discriminator value ($S_{J_b \text{ tag}}$) to be at least 0.76. The above selection criteria correspond to the working point of the CMS top quark tagging algorithm defined by a 0.3% top-quark mistagging rate [52], with a corresponding top-quark efficiency of approximately 30%.

Scale factors resulting from small differences in t tagging efficiencies in data and simulation are derived in a pure semileptonic $t\bar{t}$ sample separately for jets with p_T greater or less than 550 GeV. These are applied as corrections to simulated events, and are consistent with unity.

4.2 Identification of electrons and muons

Electron candidates are selected using a multivariate identification technique, specifically, a boosted decision tree. The multivariate discriminant is based on the spatial energy distribution of the shower, the quality of the track, the match between the track and electromagnetic cluster, the fraction of total cluster energy deposited in the HCAL, the amount of energy appearing in the regions surrounding the tracker and calorimeters, and the probability of the electron to have

originated from a converted photon. The track associated with a muon candidate is required to have hits in the pixel and muon detectors, good quality, and transverse and longitudinal impact parameters (distance of closest approach) with respect to the leading vertex close to zero.

Both the leptonic and hadronic analyses use the same criteria for muon identification, while the criteria used for electron identification are less restrictive in the hadronic analysis than in the leptonic analysis. The choice of lepton identification and use of a veto ensure that there is no overlap between events in the two analyses, and makes combining their results straightforward.

Scale factors arising from small differences between lepton identification efficiencies in data and simulation are obtained from a data sample of $Z \rightarrow \ell\ell$ events as a function of $|\eta|$. These scale factors are then applied as corrections to simulated events.

In highly boosted semileptonic top quark decays from heavy W'_R bosons, the lepton and jet may not be well separated. For this reason, no isolation requirement is applied to the lepton. Instead, a two-dimensional requirement is placed on the ΔR and p_T^{rel} for the lepton and the closest jet with $p_T > 25 \text{ GeV}$ and $|\eta| < 2.5$, where the p_T^{rel} is given by the magnitude of the component of the lepton momentum orthogonal to the jet axis. For electrons (muons), we require that either $\Delta R > 0.4$ or $p_T^{\text{rel}} > 60(50) \text{ GeV}$. These requirements help remove the multijet contribution from the background in the leptonic analysis, while maintaining high efficiency for signal events. The four-momenta of identified lepton-candidate particles are subtracted from the four-momentum of the jets that contain them, which helps ensure that jets considered in the leptonic analysis are not contaminated by nearby high-energy leptons.

4.3 Mass reconstruction

The methods of reconstructing W'_R boson candidates differ in the two analyses. In the leptonic channel, the tb invariant mass is reconstructed from the charged lepton, \vec{p}_T^{miss} , and two jets in the event. The x - and y -components of neutrino p_T are determined from \vec{p}_T^{miss} and the z -component is calculated by constraining the invariant mass of the lepton and neutrino to the mass of the W boson. This leads to a quadratic equation in p_z^{ν} . When the two solutions are real numbers, both are used to reconstruct W boson candidates. If both solutions contain imaginary parts, we set p_z^{ν} to the real part of the solutions, and recompute p_T^{ν} , which yields a different quadratic ambiguity. In the latter case, we use only the solution with mass closest to 80.4 GeV . Once we have all components of the neutrino momentum, we combine the viable neutrino momentum solutions with the charged lepton momentum to create W boson candidates. We then reconstruct the top quark by combining the four-momenta of each of the W boson candidates with each jet with $p_T > 25 \text{ GeV}$ and $|\eta| < 2.4$. Whichever jet yields a top quark candidate mass closest to 172.5 GeV is labeled as the “best jet” and is used to reconstruct the top quark candidate. In the case of two W candidates, we use the candidate that yields the top quark mass closest to its nominal value of 172.5 GeV . Finally, we combine the top quark candidate with the highest p_T jet, that is not the “best jet,” yielding the reconstructed W'_R candidate.

In the hadronic channel, the tb invariant mass is reconstructed from the two leading AK8 jets in the event.

4.4 Analysis selections in the leptonic channel

Candidate events in the leptonic analysis are selected in the HLT with single-lepton triggers that require a p_T of at least $105 (45) \text{ GeV}$ for electrons (muons) and have no isolation requirement. Scale factors to account for differences in efficiency between data and simulation are

obtained through the procedure outlined in Section 4.2. Events must contain a reconstructed lepton with $p_T > 180 \text{ GeV}$ and $|\eta| < 2.5(2.1)$ in the electron (muon) channel. Events are rejected if they contain more than one identified lepton with $p_T > 35 \text{ GeV}$ and $|\eta| < 2.5(2.1)$ in the electron (muon) channel.

Events are also required to have at least two jets with $p_T > 30 \text{ GeV}$ and $|\eta| < 2.4$, and the jet with leading p_T must have $p_T > 350(450) \text{ GeV}$ in the electron (muon) channel, where at least one of these jets must be b tagged. Events must have $\vec{p}_T^{\text{miss}} > 120(50) \text{ GeV}$ in the electron (muon) channel. In addition, events in the electron channel must have an opening angle in the transverse plane between the electron and the \vec{p}_T^{miss} vector $|\Delta\phi(e, \vec{p}_T^{\text{miss}})| < 2$ radians. In both channels, the top quark candidate is required to have $p_T^t > 250 \text{ GeV}$ and $p_T^{j_1+j_2} > 350 \text{ GeV}$, where $p_T^{j_1+j_2}$ is the p_T of the vector sum of the two leading p_T jets. In addition, in the muon channel, the mass of the top quark candidate must satisfy the condition $100 < m_t < 250 \text{ GeV}$. These requirements all serve to reject events which are not consistent with the decay of a heavy resonance to a top and bottom quark. The selections in both channels are optimized separately, thereby leading to slight differences in certain requirements. Event yields after the selection for the leptonic analysis are shown in Table 1.

Table 1: Number of selected events, and the number of signal and background events expected from simulation in the leptonic analysis. The expectations for signal and background correspond to an integrated luminosity of 2.2 fb^{-1} . “Full selection” refers to the additional requirements of $p_T^t > 250 \text{ GeV}$ and $p_T^{j_1+j_2} > 350 \text{ GeV}$ for both channels, and also $100 < m_t < 250 \text{ GeV}$ in the muon channel, while “Object selection” omits these requirements. The quoted uncertainty does not include systematic uncertainties that affect the shape of distributions (a complete description of sources of uncertainty can be found in Section 6).

	Electron channel				Muon channel			
	Object selection		Full selection		Object selection		Full selection	
	1 b tag	2 b tags	1 b tag	2 b tags	1 b tag	2 b tags	1 b tag	2 b tags
Signal								
$M_{W'_R} = 1400 \text{ GeV}$	30	22	28	20	35	31	26	24
$M_{W'_R} = 2000 \text{ GeV}$	9	6	9	6	11	9	9	7
$M_{W'_R} = 2600 \text{ GeV}$	3	1	3	1	3	2	3	1
Background								
$t\bar{t}$	71	26	56	19	68	27	49	18
tqb	5	2	4	1	4	1	3	1
tW	11	6	10	5	9	3	4	1
$\bar{t}W$	11	4	9	4	9	4	5	2
tb	1	0	1	0	0	0	0	0
$W(\rightarrow \ell\nu)+jj$	89	8	77	7	80	6	25	1
$W(\rightarrow \ell\nu)+bb/cc$	139	22	119	18	128	23	45	7
$(Z \rightarrow \ell\ell)+\text{jets}$	3	0	4	0	21	0	12	0
WW, WZ, ZZ	9	0	7	0	3	0	0	0
Total background	339±22	67±5	287±19	53±4	322±24	64±5	143±11	30±3
Data	309	58	256	44	281	58	143	30

4.5 Analysis selections in the hadronic channel

Candidate events in the hadronic channel are required to satisfy one of two HLT selections. The first demands at least two AK8 jets with $p_T > 200 \text{ GeV}$, one of which must have a trimmed [53] jet mass greater than 30 GeV , and also requires the leading p_T jet to have $p_T > 280 \text{ GeV}$.

In addition, this trigger requires that the event contains at least one b-tagged jet. The second trigger requires that the scalar p_T sum of reconstructed jets be at least 800 GeV. The efficiency of the combination of these two triggers is measured with data collected using a trigger with a lower scalar p_T sum threshold, and is extracted as a function of the scalar p_T sum of the two jets with leading p_T (H_T), which provides a way to account for this effect.

We require events to have at least two jets with $p_T > 350$ GeV, one of which must be identified as a top jet using the t tagging algorithm, and the other must be tagged as a bottom jet. Furthermore, the b jet must have a soft-drop mass less than 70 GeV. Finally, the two jets are required to be separated by $|\Delta\phi| > \pi/2$ radians and to have $|\Delta y| < 1.3$, where Δy is the rapidity difference between the two jets.

The event yields after implementing the selections in the hadronic analysis are shown in Table 2.

Table 2: Number of selected events, and the number of signal and background events expected from simulation in the hadronic analysis. The expectations for signal and background correspond to an integrated luminosity of 2.6 fb^{-1} . The quoted uncertainty does not include systematic uncertainties that affect the shape of distributions (a complete description of sources of uncertainty can be found in Section 6).

Signal	
$M_{W'_R} = 1400 \text{ GeV}$	228
$M_{W'_R} = 2000 \text{ GeV}$	27
$M_{W'_R} = 2600 \text{ GeV}$	4
Background	
Multijets	6134
$t\bar{t}$	376
tW	32
Total background	6542 ± 102
Data	6491

5 Backgrounds

5.1 Backgrounds in the leptonic analysis

5.1.1 Top quark pair production background

The predicted $t\bar{t}$ background is estimated from simulation and checked in two distinct control regions, both of which do not apply the requirements on $p_T^{j_1+j_2}$, p_T^t , m_t , nor the number of b jets. The first region is defined by relaxing the leading jet p_T and \vec{p}_T^{miss} requirements, and requiring events to have at least four jets, two of which are b-tagged, and have $400 < M_{t\bar{t}} < 750$ GeV. The latter requirement ensures that the signal contamination in this region is less than 1%. The second region is defined by requiring events to have two leptons, which must have $p_T > 150(35)$ GeV for the leading (subleading) p_T lepton. This requirement ensures that there is no overlap between the signal region and the second control region. In addition, we relax the requirements on the leading jet p_T and \vec{p}_T^{miss} , and reject events for which the invariant mass of the dilepton system (if they are of the same flavor) is between 70 and 110 GeV, which ensures that the control region does not contain a significant fraction of $Z/\gamma^* + \text{jets}$ events.

In both control regions, we compare simulated distributions and overall yields with data. We

observe significantly better agreement between data and simulation when a correction is applied to the top quark p_T spectrum in the $t\bar{t}$ simulation. The correction factor is obtained from measurements of the differential top quark p_T distribution [35]. We apply this correction factor to the $t\bar{t}$ simulation, as a function of the generator-level top quark p_T , and use the differences from the distributions without the correction as estimates of the systematic uncertainty in the expected $t\bar{t}$ background.

5.1.2 W+jets background

The prediction for the W+jets background is estimated from simulation. It is then corrected for known discrepancies in the relative fraction of W+jets events with light-flavor jets compared to bottom or charm quark jets. This correction is obtained from data using a modified event selection that does not include the requirements on $p_T^{j_1+j_2}$, p_T^t , and m_t , and also removes the requirement of a b-tagged jet. This sample is referred to as the pre-tag sample. A subset of these events, in which neither of the two leading p_T jets are b tagged, is referred to as the 0-tag sample. The 0-tag sample is dominated by the W+jets background and contains contributions from other background sources, which comprise less than 20% of the total. The difference between data and simulation in the 0-tag sample is used to obtain a first-order scale factor for W+jets light-flavor events, which is applied to the W+jets simulation, and the difference between data and simulation in the pre-tag distribution is used to calculate a first-order scale factor for W+jets heavy-flavor events. This procedure is repeated until following iterations do not cause the scale factors to shift by more than 0.1%. We also check this calculation by analytically solving the system of equations from the iteration, and confirm that the two methods yield identical results.

We require that the total number of predicted events is unaffected by the simultaneous application of the two scale factors. We assign uncertainties to these factors by repeating the procedure with the b tagging scale factors varied within their uncertainties. The procedure is identical to the procedure used in Ref. [11].

5.2 Backgrounds in the hadronic analysis

5.2.1 Multijet background

The multijet background is estimated from data, and the method is verified through simulation. The procedure uses the distribution of multijet events that fail the b tagging requirement, weighted by a transfer factor (average b tagging rate) to predict the multijet yield in the signal region.

To estimate the average b tagging rate in multijet events, we define modified t tagging criteria. Specifically, we now select events that contains jets with $\tau_3/\tau_2 > 0.75$, and shift the soft-drop jet mass window to be between 50 and 170 GeV. These requirements ensure that the control region is orthogonal to the signal region and has contributions from both signal and $t\bar{t}$ events that are less than 1%. Using the standard $S_{J_{b\text{ tag}}}$ requirement in the signal region, we favor a similar parton flavor composition. A control region is then defined by applying the signal selection with the modified t tagging requirements, omitting the b tagging requirement.

We calculate the average b tagging rate as a function of b candidate jet p_T in three $|\eta|$ regions: $|\eta| < 0.50$ (low), $0.50 \leq |\eta| < 1.15$ (transition), $1.15 \leq |\eta| < 2.40$ (high). The denominator contains all events in the control region, while the numerator includes only those that pass the signal region b tagging requirement. The average b tagging rate in each $|\eta|$ range is fitted using

a bifurcated polynomial that models the distribution. The functional form is

$$f(p_T) = \begin{cases} c_0 + c_1 p_T + c_2 (p_T - a)^2, & \text{if } p_T < a \\ c_0 + c_1 p_T + c_3 (p_T - a)^2, & \text{if } p_T \geq a. \end{cases} \quad (5)$$

The parameters c_0 to c_3 are free coefficients determined in the fit. The value of a is chosen separately for each $|\eta|$ region, and is 500, 500, and 550 GeV in the low, transition, and high- $|\eta|$ regions, respectively.

The uncertainty related to the average b tagging rate is obtained from the full covariance matrix of the fitting algorithm. The functional form is chosen to optimize agreement between sideband and Monte Carlo estimates. We estimate an uncertainty related to the choice of the fit function by comparing the results of the nominal fit with those determined using other functional forms. These other forms include the following: a constant, a second-degree polynomial, a third-degree polynomial, and an exponential function.

We observe that there is a correlation between the b tag rate and the soft-drop mass of the b candidate. To account for this correlation, we extract a correction factor for the multijet background as a function of the soft-drop mass of the b jet candidate. This factor is calculated by taking the ratio of the soft-drop mass distributions for the b tagging pass and b tagging fail samples in the control region of the multijet simulation. The factor is then used as an event weight along with the fit to the average b tagging rate to estimate the multijet background from data. An uncertainty in the factor, equal to half the difference between the factor and unity, is included in the analysis.

We check the closure of this procedure using both multijet simulation and an additional control region in data. The control region is defined by inverting the $SJ_{b \text{ tag}}$ requirement in the signal region. This provides a much purer multijet sample in data, which is orthogonal to both the signal region and the control region used to estimate the multijet contribution.

The closure test using the prediction from simulation shows a small residual discrepancy in the M_{tb} distribution, which is used to extract a correction for the multijet prediction. We include an uncertainty in this correction equal to the difference between the correction and unity. After this correction, the corresponding closure test in the data control region shows good agreement between the multijet prediction and observed data.

5.2.2 Top quark pair production background

In the hadronic analysis, the $t\bar{t}$ background prediction is estimated from simulation and checked in a region defined through selections identical to those used in the signal region, except that the b jet soft-drop mass requirement is inverted. This region contains an increased fraction of $t\bar{t}$ events relative to the signal region (approximately a factor of six), and does not overlap with the signal region or any other control regions used in the analysis. The prediction for the multijet background in this region is estimated from data using the same method as the signal region. The prediction for the $t\bar{t}$ background is found to be consistent with that observed in the data, and no other correction is required.

6 Systematic uncertainties

Systematic uncertainties fall into two categories: those that affect only the total event yield, and those that affect both the event yield and the M_{tb} distribution. Unless otherwise specified, the uncertainties are common both the leptonic and hadronic analyses.

The uncertainty in the measured integrated luminosity (2.7%) [54] belongs to the first category. The leptonic analysis includes uncertainties on the modeling of the lepton trigger (2-4%). The hadronic analysis includes uncertainties in the AK4 vs. AK8 jet b tagging rates (3%), t tagging efficiency (20%), and in the theoretical $t\bar{t}$ and single top quark cross sections ($\approx 5\%$).

Since the two analyses use the same criteria to identify muons, but different criteria for electrons, the uncertainty in the muon reconstruction and identification (2%) is included in both analyses, while the uncertainty in electron reconstruction and identification (5%) is included only in the leptonic analysis.

Other uncertainties belong to the second category and are detailed below. Unless otherwise specified, the uncertainties are assigned to all samples for which the prediction is estimated from simulation.

The uncertainties due to the choice in the renormalization and factorization scales (μ_R and μ_F , respectively) are evaluated at the matrix element level using event weights to change the scales up or down relative to the nominal scale by a factor of two, while restricting to $0.5 \leq \mu_R/\mu_F \leq 2$ [55, 56]. The uncertainty from changes in both scales at the parton shower level are evaluated for the $t\bar{t}$ background using samples generated with twice or half the nominal scale.

Uncertainties on the b tagging, jet energy scale, and jet energy resolution are calculated by varying the relevant scale factors within their uncertainties. For the jet energy scale and resolution, nominal factors and uncertainties are obtained for both AK4 and AK8 jets and applied appropriately in the leptonic and hadronic analyses.

A correction is applied to all simulated event samples to provide better matching of the distribution of pileup interactions in data. This procedure uses a minimum bias interaction cross section (σ_{mb}) of 69 mb, and uncertainties are calculated by varying the minimum bias cross section by $\pm 5\%$.

To estimate the uncertainty arising from the choice of the PDF, we use the NNPDF 3.0 PDF set uncertainty defined in Ref. [57].

In the leptonic analysis, the uncertainties in the W+jets heavy- and light-flavor factors are included as a variation in the W+jets background, and the $t\bar{t}$ background with an uncorrected top quark p_T spectrum is included as a one-sided systematic uncertainty.

In the hadronic analysis, the uncertainty in the trigger efficiency is taken to be one half of the measured trigger inefficiency, and applied as a function of the scalar p_T sum of the two leading jets. Uncertainties in the multijet background estimation procedure are also applied. These result from choice of functional form in the fit to the average b tagging rate, corrections due to correlations between the average b tagging rate and soft-drop jet mass, and differences obtained from a closure test in simulation.

In the leptonic analysis, the dominant uncertainty sources are from the correction to the p_T spectrum of the top quark in $t\bar{t}$ events, and μ_R and μ_F at the matrix element level. In the hadronic analysis, the dominant uncertainty sources are from the multijet background estimation and t tagging efficiency. Both analyses are also affected by the subdominant uncertainties related to the choice of PDF and b tagging. All systematic uncertainties for both analyses are summarized separately in Table 3.

Table 3: Sources of systematic uncertainty affecting the M_{tb} distribution taken into account when setting 95% CL upper limits. The three right-most columns indicate the channels to which the uncertainty applies (noted by \circ), and whether it also applies to signals (noted by \checkmark). When a source applies to both channels, it is treated as fully correlated in the combination. Sources that list the changes as ± 1 standard deviation (s.d.) depend on the distribution of the variable given in the parentheses, while those that list the variation as a percent are rate uncertainties.

Source	Variation	Leptonic	Hadronic	Signal
Integrated luminosity	$\pm 2.7\%$	\circ	\circ	\checkmark
Muon identification efficiency	$\pm 2\%$	\circ	\circ	\checkmark
Electron identification efficiency	$\pm 5\%$	\circ		\checkmark
Single-lepton trigger (e/μ)	$\pm 4\%/2\%$	\circ		\checkmark
AK4 to AK8 b tagging	$\pm 3\%$		\circ	\checkmark
Top quark tagging	$\pm 20\%$		\circ	\checkmark
$t\bar{t}$ cross section	$+4.8\%, -5.5\%$		\circ	
tW cross section	$\pm 5.4\%$		\circ	
Matrix element μ_R/μ_F scales	$\pm 1\text{s.d.}(\mu_R/\mu_F)$	\circ		
$t\bar{t}$ parton shower scale	$\pm 1\text{s.d.}(\mu_R/\mu_F)$	\circ	\circ	
Jet energy scale	$\pm 1\text{s.d.}(p_T, \eta)$	\circ	\circ	\checkmark
Jet energy resolution	$\pm 1\text{s.d.}(p_T, \eta)$	\circ	\circ	\checkmark
b tagging	$\pm 1\text{s.d.}(p_T)$	\circ	\circ	\checkmark
Light quark mistag rate	$\pm 1\text{s.d.}(p_T, \eta)$	\circ		\checkmark
Pileup	$\pm 1\text{s.d.}(\sigma_{mb})$	\circ	\circ	\checkmark
PDFs	$\pm 1\text{s.d.}$	\circ	\circ	\checkmark
W+jets heavy-flavor fraction	$\pm 1\text{s.d.}$	\circ		
Top p_T reweighting	$+1\text{s.d.}$	\circ		
H_T trigger	$\pm 1\text{s.d.}(H_T)$		\circ	\checkmark
Average b tagging rate fit	$\pm 1\text{s.d.}(p_T, \eta)$		\circ	
Alternative functional forms	$\pm 1\text{s.d.}(p_T, \eta)$		\circ	
b candidate mass	$\pm 1\text{s.d.}(M_b)$		\circ	
Multijet simulation nonclosure	$\pm 1\text{s.d.}(M_{tb})$		\circ	

7 Results

Comparisons of the M_{tb} distribution between the predicted background and observed data for both analyses are shown in Figs. 1 and 2. We observe good agreement between the predicted SM background processes and the observed data, and proceed to set upper limits at 95% CL on the W'_R boson production cross section for masses between 1 and 3 TeV. Limits on the cross section of W'_R boson production are calculated using a Bayesian method with a flat signal prior, using the THETA package [58]. The Bayesian approach uses a binned likelihood to calculate 95% CL upper limits on the product of the signal production cross section and the branching fraction $\sigma(\text{pp} \rightarrow W'_R) \mathcal{B}(W'_R \rightarrow t\bar{b})$. The computation takes into account all systematic uncertainties given in Section 6, as well as statistical uncertainties related to the backgrounds, which are incorporated using the “Barlow–Beeston lite” method [59, 60]. All rate uncertainties are included as nuisance parameters with log-normal priors.

The leptonic analysis separates events into four independent categories according to the lepton type (electron or muon) and the number of b-tagged jets in the first two leading p_T jets (1 or 2). This improves the sensitivity of the analysis. In the leptonic analysis, the M_{tb} distribution is binned to reduce uncertainties from the number of events in each sample. The binning is as

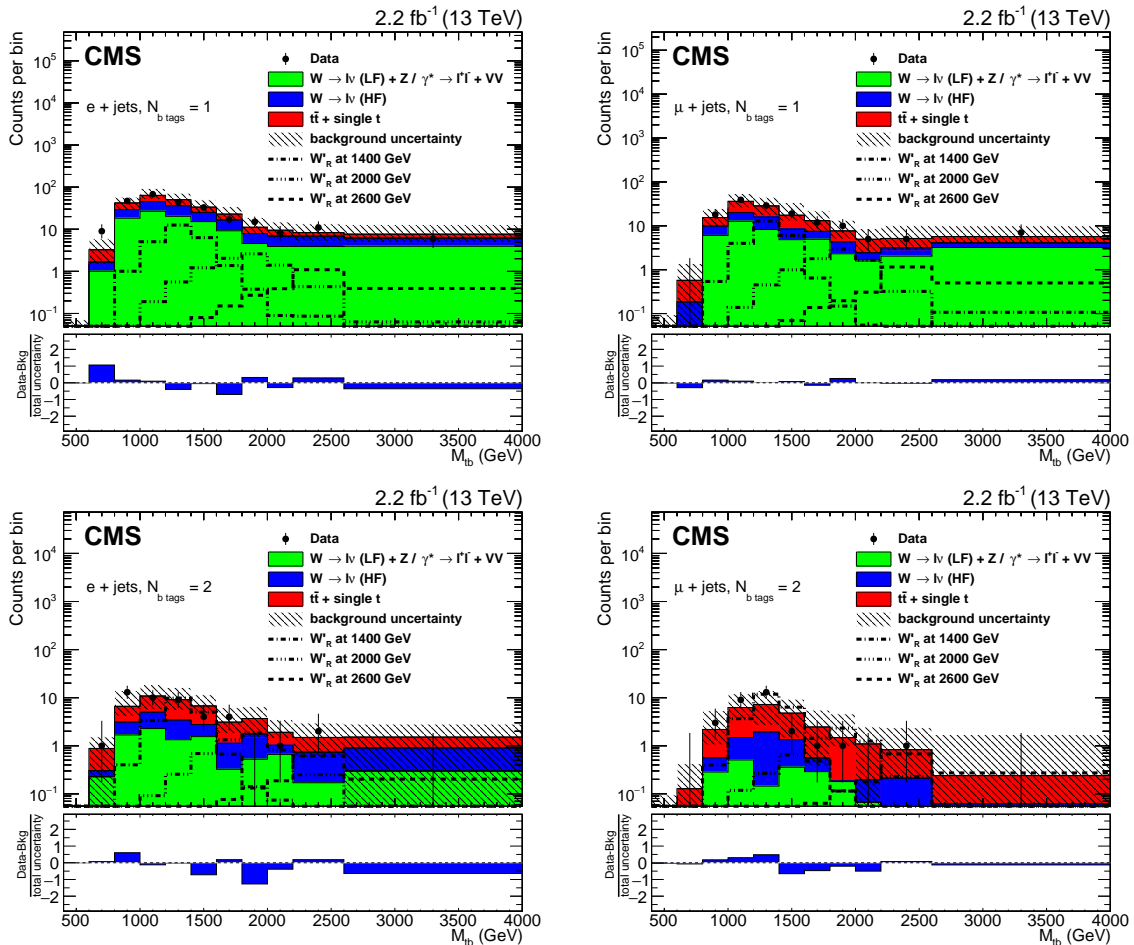


Figure 1: Reconstructed M_{tb} distributions from the leptonic analysis in the 1 b tag (upper) and 2 b tag (lower) categories, for the electron (left) and muon (right) channels. The “LF” and “HF” notations indicate the light- and heavy-flavor components of the W+jets contribution, respectively. The simulated W'_R signal and background samples are normalized to the integrated luminosity of the analyzed data set. The distributions are shown after the application of all selections. The 68% uncertainty in the background estimate includes all contributions to the predicted background, while the total uncertainty is the combined uncertainty of the background and data.

follows: 9 bins with widths of 200 GeV from 400 to 2200 GeV, 1 bin of width 400 GeV from 2200 to 2600 GeV, and 1 bin for 2600 GeV and above. In the hadronic analysis, the M_{tb} distribution is binned using 50 GeV bins from 0 to 2100 GeV, 100 GeV bins from 2100 to 2500 GeV, and 1 bin for 2500 GeV and above.

Results from the two analyses are shown separately in Fig. 3. The leptonic and hadronic analyses are able to exclude W'_R boson masses below 2.4 and 2.0 TeV, respectively.

In combining the two analyses, a joint likelihood is used to simultaneously consider all categories. We treat the uncertainties related to jet energy scale and resolution, luminosity, pileup, b tagging scale factors, and PDF as fully correlated. All other uncertainties are considered to be uncorrelated.

The combined upper limit on W'_R boson production cross section at 95% CL is shown in Fig. 4. The observed and expected 95% CL upper limits are 2.5 and 2.4 TeV, respectively. This repre-

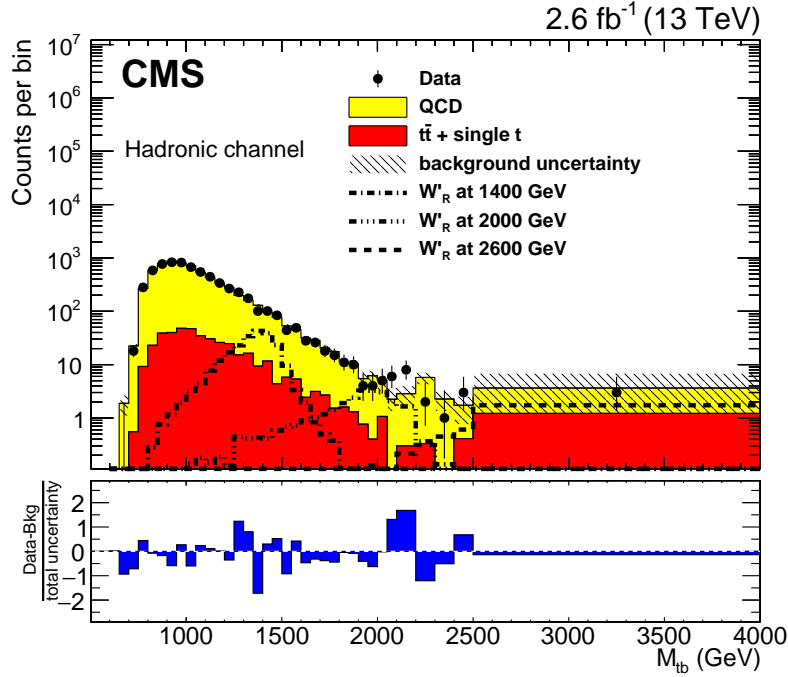


Figure 2: Reconstructed M_{tb} distribution from the hadronic analysis. The simulated W'_R signal and backgrounds are normalized to the integrated luminosity of the analyzed data set. The distribution is shown after the application of all selections. The 68% uncertainty in the background estimate includes all contributions to the predicted background, while the total uncertainty is the combined uncertainty of the background and data.

sents a significant improvement over the results from the individual analyses.

8 Summary

Searches have been reported for a heavy W'_R boson resonance decaying into a top and a bottom quark in data from proton-proton collisions at $\sqrt{s} = 13$ TeV collected with the CMS detector. Analysis of the leptonic and hadronic channels is based on an integrated luminosity of 2.2 and 2.6 fb^{-1} , respectively. No evidence is observed for the production of a W'_R boson, and upper limits at 95% confidence level on $\sigma(pp \rightarrow W'_R) \mathcal{B}(W'_R \rightarrow tb)$ are determined as a function of the W'_R boson mass. After combining the two analyses, the upper limits at 95% confidence level are compared to the predicted W'_R boson production cross sections. W'_R bosons are excluded for masses less than 2.4 TeV if $M_{W'_R} \gg M_{\nu_R}$, and less than 2.6 TeV if $M_{W'_R} < M_{\nu_R}$. These results represents the most stringent limits published in the tb decay channel.

Acknowledgments

We congratulate our colleagues in the CERN accelerator departments for the excellent performance of the LHC and thank the technical and administrative staffs at CERN and at other CMS institutes for their contributions to the success of the CMS effort. In addition, we gratefully acknowledge the computing centers and personnel of the Worldwide LHC Computing Grid for delivering so effectively the computing infrastructure essential to our analyses. Finally, we acknowledge the enduring support for the construction and operation of the LHC and the CMS detector provided by the following funding agencies: BMWFW and FWF (Aus-

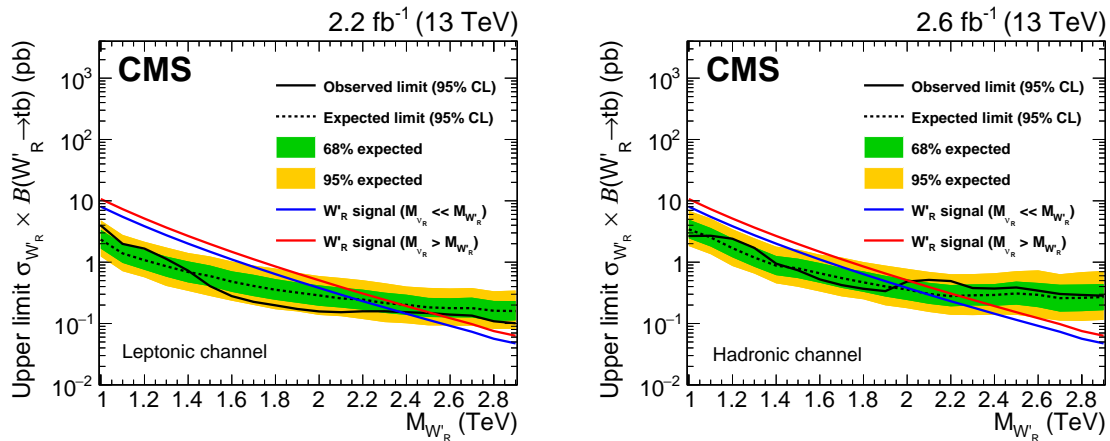


Figure 3: The 95% CL upper limit on the W'_R boson production cross section, separately for the leptonic (left) and hadronic (right) analyses. Masses for which the theoretical cross section is above the observed upper limit are excluded at 95% CL.

tria); FNRS and FWO (Belgium); CNPq, CAPES, FAPERJ, and FAPESP (Brazil); MES (Bulgaria); CERN; CAS, MoST, and NSFC (China); COLCIENCIAS (Colombia); MSES and CSF (Croatia); RPF (Cyprus); SENESCYT (Ecuador); MoER, ERC IUT, and ERDF (Estonia); Academy of Finland, MEC, and HIP (Finland); CEA and CNRS/IN2P3 (France); BMBF, DFG, and HGF (Germany); GSRT (Greece); OTKA and NIH (Hungary); DAE and DST (India); IPM (Iran); SFI (Ireland); INFN (Italy); MSIP and NRF (Republic of Korea); LAS (Lithuania); MOE and UM (Malaysia); BUAP, CINVESTAV, CONACYT, LNS, SEP, and UASLP-FAI (Mexico); MBIE (New Zealand); PAEC (Pakistan); MSHE and NSC (Poland); FCT (Portugal); JINR (Dubna); MON, RosAtom, RAS, RFBR and RAEP (Russia); MESTD (Serbia); SEIDI, CPAN, PCTI and FEDER (Spain); Swiss Funding Agencies (Switzerland); MST (Taipei); ThEPCenter, IPST, STAR, and NSTDA (Thailand); TUBITAK and TAEK (Turkey); NASU and SFFR (Ukraine); STFC (United Kingdom); DOE and NSF (USA).

Individuals have received support from the Marie-Curie program and the European Research Council and Horizon 2020 Grant, contract No. 675440 (European Union); the Leventis Foundation; the A. P. Sloan Foundation; the Alexander von Humboldt Foundation; the Belgian Federal Science Policy Office; the Fonds pour la Formation à la Recherche dans l'Industrie et dans l'Agriculture (FRIA-Belgium); the Agentschap voor Innovatie door Wetenschap en Technologie (IWT-Belgium); the Ministry of Education, Youth and Sports (MEYS) of the Czech Republic; the Council of Science and Industrial Research, India; the HOMING PLUS program of the Foundation for Polish Science, cofinanced from European Union, Regional Development Fund, the Mobility Plus program of the Ministry of Science and Higher Education, the National Science Center (Poland), contracts Harmonia 2014/14/M/ST2/00428, Opus 2014/13/B/ST2/02543, 2014/15/B/ST2/03998, and 2015/19/B/ST2/02861, Sonata-bis 2012/07/E/ST2/01406; the National Priorities Research Program by Qatar National Research Fund; the Programa Clarín-COFUND del Principado de Asturias; the Thalís and Aristeia programs cofinanced by EU-ESF and the Greek NSRF; the Rachadapisek Sompot Fund for Postdoctoral Fellowship, Chulalongkorn University and the Chulalongkorn Academic into Its 2nd Century Project Advancement Project (Thailand); and the Welch Foundation, contract C-1845.

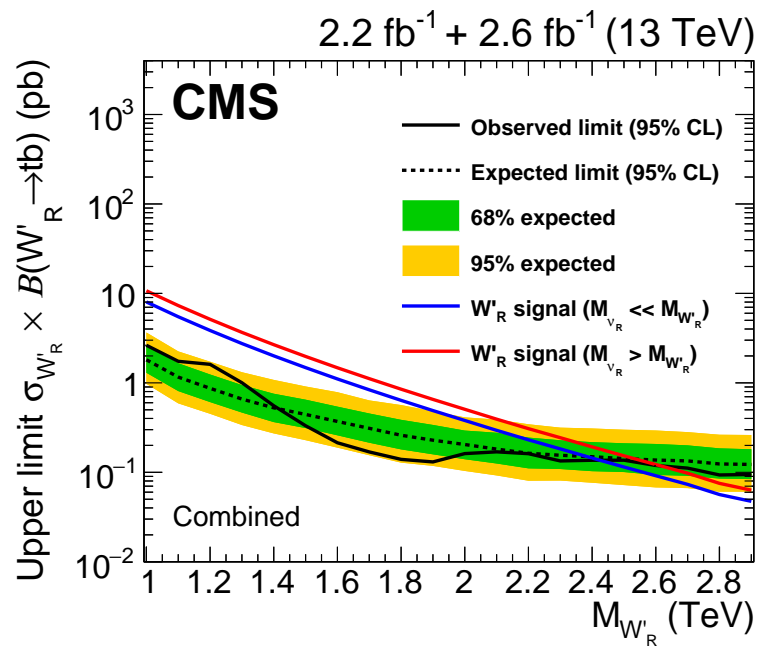


Figure 4: The 95% CL upper limit on the W'_R boson production cross section for the combined leptonic and hadronic analyses. Masses for which the theoretical cross section is above the observed upper limit are excluded at 95% CL.

References

- [1] M. Schmaltz and D. Tucker-Smith, “Little Higgs review”, *Ann. Rev. Nucl. Part. Sci.* **55** (2005) 229, doi:10.1146/annurev.nucl.55.090704.151502, arXiv:hep-ph/0502182.
- [2] T. Appelquist, H.-C. Cheng, and B. A. Dobrescu, “Bounds on universal extra dimensions”, *Phys. Rev. D* **64** (2001) 035002, doi:10.1103/PhysRevD.64.035002, arXiv:hep-ph/0012100.
- [3] H.-C. Cheng, C. T. Hill, S. Pokorski, and J. Wang, “Standard model in the latticized bulk”, *Phys. Rev. D* **64** (2001) 065007, doi:10.1103/PhysRevD.64.065007, arXiv:hep-th/0104179.
- [4] R. S. Chivukula, E. H. Simmons, and J. Terning, “Limits on noncommuting extended technicolor”, *Phys. Rev. D* **53** (1996) 5258, doi:10.1103/PhysRevD.53.5258, arXiv:hep-ph/9506427.
- [5] R. N. Mohapatra and J. C. Pati, “Left-right gauge symmetry and an ‘isoconjugate’ model of CP violation”, *Phys. Rev. D* **11** (1975) 566, doi:10.1103/PhysRevD.11.566.
- [6] D. J. Muller and S. Nandi, “Topflavor: a separate SU(2) for the third family”, *Phys. Lett. B* **383** (1996) 345, doi:10.1016/0370-2693(96)00745-9, arXiv:hep-ph/9607328.
- [7] E. Malkawi, T. Tait, and C.-P. Yuan, “A model of strong flavor dynamics for the top quark”, *Phys. Lett. B* **385** (1996) 304, doi:10.1016/0370-2693(96)00859-3, arXiv:hep-ph/9603349.
- [8] D0 Collaboration, “Search for w' boson resonances decaying to a top quark and a bottom quark”, *Phys. Rev. Lett.* **100** (2008) 211803, doi:10.1103/PhysRevLett.100.211803, arXiv:0803.3256.
- [9] D0 Collaboration, “Search for W' resonances with left- and right-handed couplings to fermions”, *Phys. Lett. B* **699** (2011) 145, doi:10.1016/j.physletb.2011.03.066, arXiv:1101.0806.
- [10] CDF Collaboration, “Search for resonances decaying to top and bottom quarks with the cdf experiment”, *Phys. Rev. Lett.* **115** (2015) 061801, doi:10.1103/PhysRevLett.115.061801, arXiv:1504.01536.
- [11] CMS Collaboration, “Search for $W' \rightarrow tb$ decays in the lepton+jets final state in pp collisions at $\sqrt{s} = 8$ TeV”, *JHEP* **05** (2014) 108, doi:10.1007/JHEP05(2014)108, arXiv:1402.2176.
- [12] CMS Collaboration, “Search for $W' \rightarrow tb$ decays in proton-proton collisions at $\sqrt{s} = 8$ TeV”, *JHEP* **02** (2016) 122, doi:10.1007/JHEP02(2016)122, arXiv:1509.06051.
- [13] ATLAS Collaboration, “Search for $W' \rightarrow t\bar{b}$ in the lepton plus jets final state in proton-proton collisions at a centre-of-mass energy of $\sqrt{s} = 8$ TeV with the ATLAS detector”, *Phys. Lett. B* **743** (2015) 235, doi:10.1016/j.physletb.2015.02.051, arXiv:1410.4103.
- [14] ATLAS Collaboration, “Search for $W' \rightarrow tb \rightarrow qqbb$ decays in pp collisions at $\sqrt{s} = 8$ TeV with the ATLAS detector”, *Eur. Phys. J. C* **75** (2015) 165, doi:10.1140/epjc/s10052-015-3372-2, arXiv:1408.0886.

- [15] CMS Collaboration, “The CMS experiment at the CERN LHC”, *JINST* **3** (2008) S08004, doi:10.1088/1748-0221/3/08/S08004.
- [16] CMS Collaboration, “Performance of electron reconstruction and selection with the CMS detector in proton-proton collisions at $\sqrt{s} = 8$ TeV”, *JINST* **10** (2015) P06005, doi:10.1088/1748-0221/10/06/P06005, arXiv:1502.02701.
- [17] CMS Collaboration, “Performance of CMS muon reconstruction in pp collision events at $\sqrt{s} = 7$ TeV”, *JINST* **7** (2012) P10002, doi:10.1088/1748-0221/7/10/P10002, arXiv:1206.4071.
- [18] CMS Collaboration, “The CMS trigger system”, *JINST* **12** (2017) P01020, doi:10.1088/1748-0221/12/01/P01020, arXiv:1609.02366.
- [19] CMS Collaboration, “Particle-flow event reconstruction in CMS and performance for jets, taus, and E_T^{miss} ”, CMS Physics Analysis Summary CMS-PAS-PFT-09-001, 2009.
- [20] CMS Collaboration, “Commissioning of the particle-flow event reconstruction with the first LHC collisions recorded in the CMS detector”, CMS Physics Analysis Summary CMS-PAS-PFT-10-001, 2010.
- [21] CMS Collaboration, “Particle-flow reconstruction and global event description with the CMS detector”, (2017). arXiv:1706.04965. Submitted to JINST.
- [22] CompHEP Collaboration, “CompHEP 4.4: Automatic computations from Lagrangians to events”, *Nucl. Instrum. Meth. A* **534** (2004) 250, doi:10.1016/j.nima.2004.07.096, arXiv:hep-ph/0403113.
- [23] Z. Sullivan, “Fully differential W' production and decay at next-to-leading order in QCD”, *Phys. Rev. D* **66** (2002) 075011, doi:10.1103/PhysRevD.66.075011, arXiv:hep-ph/0207290.
- [24] D. Duffty and Z. Sullivan, “Model independent reach for W -prime bosons at the LHC”, *Phys. Rev. D* **86** (2012) 075018, doi:10.1103/PhysRevD.86.075018, arXiv:1208.4858.
- [25] J. Alwall et al., “The automated computation of tree-level and next-to-leading order differential cross sections, and their matching to parton shower simulations”, *JHEP* **07** (2014) 079, doi:10.1007/JHEP07(2014)079, arXiv:1405.0301.
- [26] R. Frederix and S. Frixione, “Merging meets matching in MC@NLO”, *JHEP* **12** (2012) 061, doi:10.1007/JHEP12(2012)061, arXiv:1209.6215.
- [27] J. Alwall et al., “Comparative study of various algorithms for the merging of parton showers and matrix elements in hadronic collisions”, *Eur. Phys. J. C* **53** (2008) 473, doi:10.1140/epjc/s10052-007-0490-5, arXiv:0706.2569.
- [28] P. Nason, “A new method for combining NLO QCD with shower Monte Carlo algorithms”, *JHEP* **11** (2004) 040, doi:10.1088/1126-6708/2004/11/040, arXiv:hep-ph/0409146.
- [29] S. Frixione, P. Nason, and C. Oleari, “Matching NLO QCD computations with Parton Shower simulations: the POWHEG method”, *JHEP* **11** (2007) 070, doi:10.1088/1126-6708/2007/11/070.

- [30] S. Alioli, P. Nason, C. Oleari, and E. Re, “A general framework for implementing NLO calculations in shower Monte Carlo programs: the POWHEG BOX”, *JHEP* **06** (2010) 043, doi:10.1007/JHEP06(2010)043, arXiv:1002.2581.
- [31] S. Frixione, P. Nason, and G. Ridolfi, “A positive-weight next-to-leading-order Monte Carlo for heavy flavour hadroproduction”, *JHEP* **09** (2007) 126, doi:10.1088/1126-6708/2007/09/126, arXiv:0707.3088.
- [32] E. Re, “Single-top Wt -channel production matched with parton showers using the POWHEG method”, *Eur. Phys. J. C* **71** (2011) 1547, doi:10.1140/epjc/s10052-011-1547-z, arXiv:1009.2450.
- [33] T. Sjöstrand et al., “An introduction to PYTHIA 8.2”, *Comput. Phys. Commun.* **191** (2015) 159, doi:10.1016/j.cpc.2015.01.024, arXiv:1410.3012.
- [34] NNPDF Collaboration, “Parton distributions for the LHC Run II”, *JHEP* **04** (2015) 040, doi:10.1007/JHEP04(2015)040, arXiv:1410.8849.
- [35] CMS Collaboration, “Measurement of the differential cross section for top quark pair production in pp collisions at $\sqrt{s} = 8$ TeV”, *Eur. Phys. J. C* **75** (2015) 542, doi:10.1140/epjc/s10052-015-3709-x, arXiv:1505.04480.
- [36] CMS Collaboration, “Measurement of the $t\bar{t}$ production cross section in pp collisions at 7 TeV in lepton+jets events using b-quark jet identification”, *Phys. Rev. D* **84** (2011) 092004, doi:10.1103/PhysRevD.84.092004, arXiv:1108.3773.
- [37] CMS Collaboration, “Event generator tunes obtained from underlying event and multiparton scattering measurements”, *Eur. Phys. J. C* **76** (2016) 155, doi:10.1140/epjc/s10052-016-3988-x, arXiv:1512.00815.
- [38] S. J. Allison et al., “Geant4 developments and applications”, *IEEE Trans. Nucl. Sci.* **53** (2006) 270, doi:10.1109/TNS.2006.869826.
- [39] M. Cacciari, G. P. Salam, and G. Soyez, “The anti- k_t jet clustering algorithm”, *JHEP* **04** (2008) 063, doi:10.1088/1126-6708/2008/04/063, arXiv:0802.1189.
- [40] M. Cacciari, G. P. Salam, and G. Soyez, “FastJet user manual”, *Eur. Phys. J. C* **72** (2012) 1896, doi:10.1140/epjc/s10052-012-1896-2, arXiv:1111.6097.
- [41] CMS Collaboration, “Determination of jet energy calibration and transverse momentum resolution in CMS”, *JINST* **6** (2011) P11002, doi:10.1088/1748-0221/6/11/P11002, arXiv:1107.4277.
- [42] M. Cacciari and G. P. Salam, “Pileup subtraction using jet areas”, *Phys. Lett. B* **659** (2008) 119, doi:10.1016/j.physletb.2007.09.077, arXiv:0707.1378.
- [43] CMS Collaboration, “Identification of b-quark jets with the CMS experiment”, *JINST* **8** (2013) P04013, doi:10.1088/1748-0221/8/04/P04013, arXiv:1211.4462.
- [44] CMS Collaboration, “Identification of b quark jets at the CMS Experiment in the LHC Run 2”, CMS Physics Analysis Summary CMS-PAS-BTV-15-001, 2015.
- [45] J. Thaler and K. Van Tilburg, “Identifying boosted objects with N-subjettiness”, *JHEP* **03** (2011) 015, doi:10.1007/JHEP03(2011)015, arXiv:1011.2268.

- [46] J. Thaler and K. Van Tilburg, “Maximizing boosted top identification by minimizing N-subjettiness”, *JHEP* **02** (2012) 093, doi:10.1007/JHEP02(2012)093, arXiv:1108.2701.
- [47] M. Dasgupta, A. Fregoso, S. Marzani, and G. P. Salam, “Towards an understanding of jet substructure”, *JHEP* **09** (2013) 029, doi:10.1007/JHEP09(2013)029, arXiv:1307.0007.
- [48] A. J. Larkoski, S. Marzani, G. Soyez, and J. Thaler, “Soft drop”, *JHEP* **05** (2014) 146, doi:10.1007/JHEP05(2014)146, arXiv:1402.2657.
- [49] Y. L. Dokshitzer, G. D. Leder, S. Moretti, and B. R. Webber, “Better jet clustering algorithms”, *JHEP* **08** (1997) 001, doi:10.1088/1126-6708/1997/08/001, arXiv:hep-ph/9707323.
- [50] M. Dasgupta, A. Fregoso, S. Marzani, and A. Powling, “Jet substructure with analytical methods”, *Eur. Phys. J. C* **73** (2013) 2623, doi:10.1140/epjc/s10052-013-2623-3, arXiv:1307.0013.
- [51] S. D. Ellis and D. E. Soper, “Successive combination jet algorithm for hadron collisions”, *Phys. Rev. D* **48** (1993) 3160, doi:10.1103/PhysRevD.48.3160, arXiv:hep-ph/9305266.
- [52] CMS Collaboration, “Top tagging with new approaches”, CMS Physics Analysis Summary CMS-PAS-JME-15-002, 2016.
- [53] D. Krohn, J. Thaler, and L.-T. Wang, “Jet trimming”, *JHEP* **02** (2010) 84, doi:10.1007/JHEP02(2010)084, arXiv:0912.1342.
- [54] CMS Collaboration, “CMS luminosity measurement for the 2015 data taking period”, CMS Physics Analysis Summary CMS-PAS-LUM-15-001, 2015.
- [55] M. Cacciari et al., “The $t\bar{t}$ cross-section at 1.8 TeV and 1.96 TeV: a study of the systematics due to parton densities and scale dependence”, *JHEP* **04** (2004) 068, doi:10.1088/1126-6708/2004/04/068, arXiv:hep-ph/0303085.
- [56] S. Catani, D. de Florian, M. Grazzini, and P. Nason, “Soft gluon resummation for Higgs boson production at hadron colliders”, *JHEP* **07** (2003) 028, doi:10.1088/1126-6708/2003/07/028, arXiv:hep-ph/0306211.
- [57] M. Botje et al., “The PDF4LHC Working Group Interim Recommendations”, (2011). arXiv:1101.0538.
- [58] T. Müller, J. Ott, and J. Wagner-Kuhr, “theta - a framework for template-based modeling and inference”, 2010.
- [59] R. Barlow and C. Beeston, “Fitting using finite Monte Carlo samples”, *Comp. Phys. Comm.* **77** (1993) 219, doi:10.1016/0010-4655(93)90005-W.
- [60] J. S. Conway, “Incorporating nuisance parameters in likelihoods for multisource spectra”, in *Proceedings, PHYSTAT 2011 Workshop on Statistical Issues Related to Discovery Claims in Search Experiments and Unfolding*, p. 115. CERN, Geneva, Switzerland, January, 2011. arXiv:1103.0354. doi:10.5170/CERN-2011-006.115.

A The CMS Collaboration

Yerevan Physics Institute, Yerevan, Armenia

A.M. Sirunyan, A. Tumasyan

Institut für Hochenergiephysik, Wien, Austria

W. Adam, F. Ambrogio, E. Asilar, T. Bergauer, J. Brandstetter, E. Brondolin, M. Dragicevic, J. Erö, M. Flechl, M. Friedl, R. Frühwirth¹, V.M. Ghete, J. Grossmann, N. Hörmann, J. Hrubec, M. Jeitler¹, A. König, I. Krätschmer, D. Liko, T. Madlener, T. Matsushita, I. Mikulec, E. Pree, D. Rabady, N. Rad, H. Rohringer, J. Schieck¹, M. Spanring, D. Spitzbart, J. Strauss, W. Waltenberger, J. Wittmann, C.-E. Wulz¹, M. Zarucki

Institute for Nuclear Problems, Minsk, Belarus

V. Chekhovsky, V. Mossolov, J. Suarez Gonzalez

National Centre for Particle and High Energy Physics, Minsk, Belarus

N. Shumeiko

Universiteit Antwerpen, Antwerpen, Belgium

E.A. De Wolf, X. Janssen, J. Lauwers, M. Van De Klundert, H. Van Haevermaet, P. Van Mechelen, N. Van Remortel, A. Van Spilbeeck

Vrije Universiteit Brussel, Brussel, Belgium

S. Abu Zeid, F. Blekman, J. D'Hondt, I. De Bruyn, J. De Clercq, K. Deroover, S. Lowette, S. Moortgat, L. Moreels, A. Olbrechts, Q. Python, K. Skovpen, S. Tavernier, W. Van Doninck, P. Van Mulders, I. Van Parijs

Université Libre de Bruxelles, Bruxelles, Belgium

H. Brun, B. Clerbaux, G. De Lentdecker, H. Delannoy, G. Fasanella, L. Favart, R. Goldouzian, A. Grebenyuk, G. Karapostoli, T. Lenzi, J. Luetic, T. Maerschalk, A. Marinov, A. Randle-conde, T. Seva, C. Vander Velde, P. Vanlaer, D. Vannerom, R. Yonamine, F. Zenoni, F. Zhang²

Ghent University, Ghent, Belgium

A. Cimmino, T. Cornelis, D. Dobur, A. Fagot, M. Gul, I. Khvastunov, D. Poyraz, S. Salva, R. Schöfbeck, M. Tytgat, W. Van Driessche, W. Verbeke, N. Zaganidis

Université Catholique de Louvain, Louvain-la-Neuve, Belgium

H. Bakhshiansohi, O. Bondu, S. Brochet, G. Bruno, A. Caudron, S. De Visscher, C. Delaere, M. Delcourt, B. Francois, A. Giammanco, A. Jafari, M. Komm, G. Krintiras, V. Lemaitre, A. Magitteri, A. Mertens, M. Musich, K. Piotrkowski, L. Quertenmont, M. Vidal Marono, S. Wertz

Université de Mons, Mons, Belgium

N. Bely

Centro Brasileiro de Pesquisas Fisicas, Rio de Janeiro, Brazil

W.L. Aldá Júnior, F.L. Alves, G.A. Alves, L. Brito, C. Hensel, A. Moraes, M.E. Pol, P. Rebello Teles

Universidade do Estado do Rio de Janeiro, Rio de Janeiro, Brazil

E. Belchior Batista Das Chagas, W. Carvalho, J. Chinellato³, A. Custódio, E.M. Da Costa, G.G. Da Silveira⁴, D. De Jesus Damiao, S. Fonseca De Souza, L.M. Huertas Guativa, H. Malbouisson, C. Mora Herrera, L. Mundim, H. Nogima, A. Santoro, A. Sznajder, E.J. Tonelli Manganote³, F. Torres Da Silva De Araujo, A. Vilela Pereira

Universidade Estadual Paulista ^a, Universidade Federal do ABC ^b, São Paulo, Brazil

S. Ahuja^a, C.A. Bernardes^a, T.R. Fernandez Perez Tomei^a, E.M. Gregores^b, P.G. Mercadante^b, C.S. Moon^a, S.F. Novaes^a, Sandra S. Padula^a, D. Romero Abad^b, J.C. Ruiz Vargas^a

Institute for Nuclear Research and Nuclear Energy, Sofia, Bulgaria

A. Aleksandrov, R. Hadjiiska, P. Iaydjiev, M. Misheva, M. Rodozov, S. Stoykova, G. Sultanov, M. Vutova

University of Sofia, Sofia, Bulgaria

A. Dimitrov, I. Glushkov, L. Litov, B. Pavlov, P. Petkov

Beihang University, Beijing, China

W. Fang⁵, X. Gao⁵

Institute of High Energy Physics, Beijing, China

M. Ahmad, J.G. Bian, G.M. Chen, H.S. Chen, M. Chen, Y. Chen, C.H. Jiang, D. Leggat, Z. Liu, F. Romeo, S.M. Shaheen, A. Spiezia, J. Tao, C. Wang, Z. Wang, E. Yazgan, H. Zhang, J. Zhao

State Key Laboratory of Nuclear Physics and Technology, Peking University, Beijing, China

Y. Ban, G. Chen, Q. Li, S. Liu, Y. Mao, S.J. Qian, D. Wang, Z. Xu

Universidad de Los Andes, Bogota, Colombia

C. Avila, A. Cabrera, L.F. Chaparro Sierra, C. Florez, C.F. González Hernández, J.D. Ruiz Alvarez

University of Split, Faculty of Electrical Engineering, Mechanical Engineering and Naval Architecture, Split, Croatia

N. Godinovic, D. Lelas, I. Puljak, P.M. Ribeiro Cipriano, T. Sculac

University of Split, Faculty of Science, Split, Croatia

Z. Antunovic, M. Kovac

Institute Rudjer Boskovic, Zagreb, Croatia

V. Brigljevic, D. Ferencek, K. Kadija, B. Mesic, T. Susa

University of Cyprus, Nicosia, Cyprus

M.W. Ather, A. Attikis, G. Mavromanolakis, J. Mousa, C. Nicolaou, F. Ptochos, P.A. Razis, H. Rykaczewski

Charles University, Prague, Czech Republic

M. Finger⁶, M. Finger Jr.⁶

Universidad San Francisco de Quito, Quito, Ecuador

E. Carrera Jarrin

Academy of Scientific Research and Technology of the Arab Republic of Egypt, Egyptian Network of High Energy Physics, Cairo, Egypt

A.A. Abdelalim^{7,8}, Y. Mohammed⁹, E. Salama^{10,11}

National Institute of Chemical Physics and Biophysics, Tallinn, Estonia

R.K. Dewanjee, M. Kadastik, L. Perrini, M. Raidal, A. Tiko, C. Veelken

Department of Physics, University of Helsinki, Helsinki, Finland

P. Eerola, J. Pekkanen, M. Voutilainen

Helsinki Institute of Physics, Helsinki, Finland

J. Härkönen, T. Järvinen, V. Karimäki, R. Kinnunen, T. Lampén, K. Lassila-Perini, S. Lehti, T. Lindén, P. Luukka, E. Tuominen, J. Tuominiemi, E. Tuovinen

Lappeenranta University of Technology, Lappeenranta, Finland

J. Talvitie, T. Tuuva

IRFU, CEA, Université Paris-Saclay, Gif-sur-Yvette, France

M. Besancon, F. Couderc, M. Dejardin, D. Denegri, J.L. Faure, F. Ferri, S. Ganjour, S. Ghosh, A. Givernaud, P. Gras, G. Hamel de Monchenault, P. Jarry, I. Kucher, E. Locci, M. Machet, J. Malcles, J. Rander, A. Rosowsky, M.Ö. Sahin, M. Titov

Laboratoire Leprince-Ringuet, Ecole polytechnique, CNRS/IN2P3, Université Paris-Saclay, Palaiseau, France

A. Abdulsalam, I. Antropov, S. Baffioni, F. Beaudette, P. Busson, L. Cadamuro, E. Chapon, C. Charlot, O. Davignon, R. Granier de Cassagnac, M. Jo, S. Lisniak, A. Lobanov, M. Nguyen, C. Ochando, G. Ortona, P. Paganini, P. Pigard, S. Regnard, R. Salerno, Y. Sirois, A.G. Stahl Leiton, T. Strebler, Y. Yilmaz, A. Zabi, A. Zghiche

Université de Strasbourg, CNRS, IPHC UMR 7178, F-67000 Strasbourg, France

J.-L. Agram¹², J. Andrea, D. Bloch, J.-M. Brom, M. Buttignol, E.C. Chabert, N. Chanon, C. Collard, E. Conte¹², X. Coubez, J.-C. Fontaine¹², D. Gelé, U. Goerlach, A.-C. Le Bihan, P. Van Hove

Centre de Calcul de l'Institut National de Physique Nucleaire et de Physique des Particules, CNRS/IN2P3, Villeurbanne, France

S. Gadrat

Université de Lyon, Université Claude Bernard Lyon 1, CNRS-IN2P3, Institut de Physique Nucléaire de Lyon, Villeurbanne, France

S. Beauceron, C. Bernet, G. Boudoul, R. Chierici, D. Contardo, B. Courbon, P. Depasse, H. El Mamouni, J. Fay, L. Finco, S. Gascon, M. Gouzevitch, G. Grenier, B. Ille, F. Lagarde, I.B. Laktineh, M. Lethuillier, L. Mirabito, A.L. Pequegnot, S. Perries, A. Popov¹³, V. Sordini, M. Vander Donckt, S. Viret

Georgian Technical University, Tbilisi, Georgia

T. Toriashvili¹⁴

Tbilisi State University, Tbilisi, Georgia

Z. Tsamalaidze⁶

RWTH Aachen University, I. Physikalisches Institut, Aachen, Germany

C. Autermann, S. Beranek, L. Feld, M.K. Kiesel, K. Klein, M. Lipinski, M. Preuten, C. Schomakers, J. Schulz, T. Verlage

RWTH Aachen University, III. Physikalisches Institut A, Aachen, Germany

A. Albert, M. Brodski, E. Dietz-Laursonn, D. Duchardt, M. Endres, M. Erdmann, S. Erdweg, T. Esch, R. Fischer, A. Güth, M. Hamer, T. Hebbeker, C. Heidemann, K. Hoepfner, S. Knutzen, M. Merschmeyer, A. Meyer, P. Millet, S. Mukherjee, M. Olschewski, K. Padeken, T. Pook, M. Radziej, H. Reithler, M. Rieger, F. Scheuch, L. Sonnenschein, D. Teysier, S. Thüer

RWTH Aachen University, III. Physikalisches Institut B, Aachen, Germany

G. Flügge, B. Kargoll, T. Kress, A. Künsken, J. Lingemann, T. Müller, A. Nehr Korn, A. Nowack, C. Pistone, O. Pooth, A. Stahl¹⁵

Deutsches Elektronen-Synchrotron, Hamburg, Germany

M. Aldaya Martin, T. Arndt, C. Asawatrangkuldee, K. Beernaert, O. Behnke, U. Behrens, A.A. Bin Anuar, K. Borras¹⁶, V. Botta, A. Campbell, P. Connor, C. Contreras-Campana, F. Costanza, C. Diez Pardos, G. Eckerlin, D. Eckstein, T. Eichhorn, E. Eren, E. Gallo¹⁷, J. Garay Garcia, A. Geiser, A. Gizhko, J.M. Grados Luyando, A. Grohsjean, P. Gunnellini, A. Harb, J. Hauk, M. Hempel¹⁸, H. Jung, A. Kalogeropoulos, M. Kasemann, J. Keaveney, C. Kleinwort, I. Korol, D. Krücker, W. Lange, A. Lelek, T. Lenz, J. Leonard, K. Lipka, W. Lohmann¹⁸, R. Mankel, I.-A. Melzer-Pellmann, A.B. Meyer, G. Mittag, J. Mnich, A. Mussgiller, E. Ntomari, D. Pitzl, R. Placakyte, A. Raspereza, B. Roland, M. Savitskyi, P. Saxena, R. Shevchenko, S. Spannagel, N. Stefaniuk, G.P. Van Onsem, R. Walsh, Y. Wen, K. Wichmann, C. Wissing

University of Hamburg, Hamburg, Germany

S. Bein, V. Blobel, M. Centis Vignali, A.R. Draeger, T. Dreyer, E. Garutti, D. Gonzalez, J. Haller, M. Hoffmann, A. Junkes, R. Klanner, R. Kogler, N. Kovalchuk, S. Kurz, T. Lapsien, I. Marchesini, D. Marconi, M. Meyer, M. Niedziela, D. Nowatschin, F. Pantaleo¹⁵, T. Peiffer, A. Perieanu, C. Scharf, P. Schleper, A. Schmidt, S. Schumann, J. Schwandt, J. Sonneveld, H. Stadie, G. Steinbrück, F.M. Stober, M. Stöver, H. Tholen, D. Troendle, E. Usai, L. Vanelderen, A. Vanhoefer, B. Vormwald

Institut für Experimentelle Kernphysik, Karlsruhe, Germany

M. Akbiyik, C. Barth, S. Baur, C. Baus, J. Berger, E. Butz, R. Caspart, T. Chwalek, F. Colombo, W. De Boer, A. Dierlamm, B. Freund, R. Friese, M. Giffels, A. Gilbert, D. Haitz, F. Hartmann¹⁵, S.M. Heindl, U. Husemann, F. Kassel¹⁵, S. Kudella, H. Mildner, M.U. Mozer, Th. Müller, M. Plagge, G. Quast, K. Rabbertz, M. Schröder, I. Shvetsov, G. Sieber, H.J. Simonis, R. Ulrich, S. Wayand, M. Weber, T. Weiler, S. Williamson, C. Wöhrmann, R. Wolf

Institute of Nuclear and Particle Physics (INPP), NCSR Demokritos, Aghia Paraskevi, Greece

G. Anagnostou, G. Daskalakis, T. Geralis, V.A. Giakoumopoulou, A. Kyriakis, D. Loukas, I. Topsis-Giotis

National and Kapodistrian University of Athens, Athens, Greece

S. Kesisoglou, A. Panagiotou, N. Saoulidou

University of Ioánnina, Ioánnina, Greece

I. Evangelou, G. Flouris, C. Foudas, P. Kokkas, N. Manthos, I. Papadopoulos, E. Paradas, J. Strologas, F.A. Triantis

MTA-ELTE Lendület CMS Particle and Nuclear Physics Group, Eötvös Loránd University, Budapest, Hungary

M. Csanad, N. Filipovic, G. Pasztor

Wigner Research Centre for Physics, Budapest, Hungary

G. Bencze, C. Hajdu, D. Horvath¹⁹, F. Sikler, V. Veszpremi, G. Vesztergombi²⁰, A.J. Zsigmond

Institute of Nuclear Research ATOMKI, Debrecen, Hungary

N. Beni, S. Czellar, J. Karancsi²¹, A. Makovec, J. Molnar, Z. Szillasi

Institute of Physics, University of Debrecen, Debrecen, Hungary

M. Bartók²⁰, P. Raics, Z.L. Trocsanyi, B. Ujvari

Indian Institute of Science (IISc), Bangalore, India

S. Choudhury, J.R. Komaragiri

National Institute of Science Education and Research, Bhubaneswar, India

S. Bahinipati²², S. Bhowmik, P. Mal, K. Mandal, A. Nayak²³, D.K. Sahoo²², N. Sahoo, S.K. Swain

Panjab University, Chandigarh, India

S. Bansal, S.B. Beri, V. Bhatnagar, U. Bhawandeep, R. Chawla, N. Dhingra, A.K. Kalsi, A. Kaur, M. Kaur, R. Kumar, P. Kumari, A. Mehta, M. Mittal, J.B. Singh, G. Walia

University of Delhi, Delhi, India

Ashok Kumar, Aashaq Shah, A. Bhardwaj, S. Chauhan, B.C. Choudhary, R.B. Garg, S. Keshri, A. Kumar, S. Malhotra, M. Naimuddin, K. Ranjan, R. Sharma, V. Sharma

Saha Institute of Nuclear Physics, HBNI, Kolkata, India

R. Bhardwaj, R. Bhattacharya, S. Bhattacharya, S. Dey, S. Dutt, S. Dutta, S. Ghosh, N. Majumdar, A. Modak, K. Mondal, S. Mukhopadhyay, S. Nandan, A. Purohit, A. Roy, D. Roy, S. Roy Chowdhury, S. Sarkar, M. Sharan, S. Thakur

Indian Institute of Technology Madras, Madras, India

P.K. Behera

Bhabha Atomic Research Centre, Mumbai, India

R. Chudasama, D. Dutta, V. Jha, V. Kumar, A.K. Mohanty¹⁵, P.K. Netrakanti, L.M. Pant, P. Shukla, A. Topkar

Tata Institute of Fundamental Research-A, Mumbai, India

T. Aziz, S. Dugad, B. Mahakud, S. Mitra, G.B. Mohanty, B. Parida, N. Sur, B. Sutar

Tata Institute of Fundamental Research-B, Mumbai, India

S. Banerjee, S. Bhattacharya, S. Chatterjee, P. Das, M. Guhait, Sa. Jain, S. Kumar, M. Maity²⁴, G. Majumder, K. Mazumdar, T. Sarkar²⁴, N. Wickramage²⁵

Indian Institute of Science Education and Research (IISER), Pune, India

S. Chauhan, S. Dube, V. Hegde, A. Kapoor, K. Kothekar, S. Pandey, A. Rane, S. Sharma

Institute for Research in Fundamental Sciences (IPM), Tehran, Iran

S. Chenarani²⁶, E. Eskandari Tadavani, S.M. Etesami²⁶, M. Khakzad, M. Mohammadi Najafabadi, M. Naseri, S. Paktinat Mehdiabadi²⁷, F. Rezaei Hosseinabadi, B. Safarzadeh²⁸, M. Zeinali

University College Dublin, Dublin, Ireland

M. Felcini, M. Grunewald

INFN Sezione di Bari ^a, Università di Bari ^b, Politecnico di Bari ^c, Bari, Italy

M. Abbrescia^{a,b}, C. Calabria^{a,b}, C. Caputo^{a,b}, A. Colaleo^a, D. Creanza^{a,c}, L. Cristella^{a,b}, N. De Filippis^{a,c}, M. De Palma^{a,b}, L. Fiore^a, G. Iaselli^{a,c}, G. Maggi^{a,c}, M. Maggi^a, G. Miniello^{a,b}, S. My^{a,b}, S. Nuzzo^{a,b}, A. Pompili^{a,b}, G. Pugliese^{a,c}, R. Radogna^{a,b}, A. Ranieri^a, G. Selvaggi^{a,b}, A. Sharma^a, L. Silvestris^{a,15}, R. Venditti^a, P. Verwilligen^a

INFN Sezione di Bologna ^a, Università di Bologna ^b, Bologna, Italy

G. Abbiendi^a, C. Battilana, D. Bonacorsi^{a,b}, S. Braibant-Giacomelli^{a,b}, L. Brigliadori^{a,b}, R. Campanini^{a,b}, P. Capiluppi^{a,b}, A. Castro^{a,b}, F.R. Cavallo^a, S.S. Chhibra^{a,b}, M. Cuffiani^{a,b}, G.M. Dallavalle^a, F. Fabbri^a, A. Fanfani^{a,b}, D. Fasanella^{a,b}, P. Giacomelli^a, L. Guiducci^{a,b}, S. Marcellini^a, G. Masetti^a, F.L. Navarria^{a,b}, A. Perrotta^a, A.M. Rossi^{a,b}, T. Rovelli^{a,b}, G.P. Siroli^{a,b}, N. Tosi^{a,b,15}

INFN Sezione di Catania ^a, Università di Catania ^b, Catania, Italy

S. Albergo^{a,b}, S. Costa^{a,b}, A. Di Mattia^a, F. Giordano^{a,b}, R. Potenza^{a,b}, A. Tricomi^{a,b}, C. Tuve^{a,b}

INFN Sezione di Firenze ^a, Università di Firenze ^b, Firenze, Italy

G. Barbagli^a, K. Chatterjee^{a,b}, V. Ciulli^{a,b}, C. Civinini^a, R. D'Alessandro^{a,b}, E. Focardi^{a,b}, P. Lenzi^{a,b}, M. Meschini^a, S. Paoletti^a, L. Russo^{a,29}, G. Sguazzoni^a, D. Strom^a, L. Viliani^{a,b,15}

INFN Laboratori Nazionali di Frascati, Frascati, Italy

L. Benussi, S. Bianco, F. Fabbri, D. Piccolo, F. Primavera¹⁵

INFN Sezione di Genova ^a, Università di Genova ^b, Genova, Italy

V. Calvelli^{a,b}, F. Ferro^a, E. Robutti^a, S. Tosi^{a,b}

INFN Sezione di Milano-Bicocca ^a, Università di Milano-Bicocca ^b, Milano, Italy

L. Brianza^{a,b}, F. Brivio^{a,b}, V. Ciriolo^{a,b}, M.E. Dinardo^{a,b}, S. Fiorendi^{a,b}, S. Gennai^a, A. Ghezzi^{a,b}, P. Govoni^{a,b}, M. Malberti^{a,b}, S. Malvezzi^a, R.A. Manzoni^{a,b}, D. Menasce^a, L. Moroni^a, M. Paganoni^{a,b}, K. Pauwels^{a,b}, D. Pedrini^a, S. Pigazzini^{a,b,30}, S. Ragazzi^{a,b}, T. Tabarelli de Fatis^{a,b}

INFN Sezione di Napoli ^a, Università di Napoli 'Federico II' ^b, Napoli, Italy, Università della Basilicata ^c, Potenza, Italy, Università G. Marconi ^d, Roma, Italy

S. Buontempo^a, N. Cavallo^{a,c}, S. Di Guida^{a,d,15}, F. Fabozzi^{a,c}, F. Fienga^{a,b}, A.O.M. Iorio^{a,b}, W.A. Khan^a, L. Lista^a, S. Meola^{a,d,15}, P. Paolucci^{a,15}, C. Sciacca^{a,b}, F. Thyssen^a

INFN Sezione di Padova ^a, Università di Padova ^b, Padova, Italy, Università di Trento ^c, Trento, Italy

P. Azzi^{a,15}, N. Bacchetta^a, S. Badoer^a, L. Benato^{a,b}, A. Boletti^{a,b}, R. Carlin^{a,b}, A. Carvalho Antunes De Oliveira^{a,b}, P. Checchia^a, M. Dall'Osso^{a,b}, P. De Castro Manzano^a, T. Dorigo^a, U. Gasparini^{a,b}, A. Gozzelino^a, S. Lacaprara^a, M. Margoni^{a,b}, A.T. Meneguzzo^{a,b}, M. Pegoraro^a, N. Pozzobon^{a,b}, P. Ronchese^{a,b}, R. Rossin^{a,b}, F. Simonetto^{a,b}, E. Torassa^a, S. Ventura^a, M. Zanetti^{a,b}, P. Zotto^{a,b}, G. Zumerle^{a,b}

INFN Sezione di Pavia ^a, Università di Pavia ^b, Pavia, Italy

A. Braghieri^a, F. Fallavollita^{a,b}, A. Magnani^{a,b}, P. Montagna^{a,b}, S.P. Ratti^{a,b}, V. Re^a, M. Ressegotti, C. Riccardi^{a,b}, P. Salvini^a, I. Vai^{a,b}, P. Vitulo^{a,b}

INFN Sezione di Perugia ^a, Università di Perugia ^b, Perugia, Italy

L. Alunni Solestizi^{a,b}, G.M. Bilei^a, D. Ciangottini^{a,b}, L. Fanò^{a,b}, P. Lariccia^{a,b}, R. Leonardi^{a,b}, G. Mantovani^{a,b}, V. Mariani^{a,b}, M. Menichelli^a, A. Saha^a, A. Santocchia^{a,b}, D. Spiga

INFN Sezione di Pisa ^a, Università di Pisa ^b, Scuola Normale Superiore di Pisa ^c, Pisa, Italy

K. Androsov^a, P. Azzurri^{a,15}, G. Bagliesi^a, J. Bernardini^a, T. Boccali^a, L. Borrello, R. Castaldi^a, M.A. Ciocci^{a,b}, R. Dell'Orso^a, G. Fedi^a, A. Giassi^a, M.T. Grippo^{a,29}, F. Ligabue^{a,c}, T. Lomtadze^a, L. Martini^{a,b}, A. Messineo^{a,b}, F. Palla^a, A. Rizzi^{a,b}, A. Savoy-Navarro^{a,31}, P. Spagnolo^a, R. Tenchini^a, G. Tonelli^{a,b}, A. Venturi^a, P.G. Verdini^a

INFN Sezione di Roma ^a, Sapienza Università di Roma ^b, Rome, Italy

L. Barone^{a,b}, F. Cavallari^a, M. Cipriani^{a,b}, D. Del Re^{a,b,15}, M. Diemoz^a, S. Gelli^{a,b}, E. Longo^{a,b}, F. Margaroli^{a,b}, B. Marzocchi^{a,b}, P. Meridiani^a, G. Organtini^{a,b}, R. Paramatti^{a,b}, F. Preiato^{a,b}, S. Rahatlou^{a,b}, C. Rovelli^a, F. Santanastasio^{a,b}

INFN Sezione di Torino ^a, Università di Torino ^b, Torino, Italy, Università del Piemonte Orientale ^c, Novara, Italy

N. Amapane^{a,b}, R. Arcidiacono^{a,c,15}, S. Argiro^{a,b}, M. Arneodo^{a,c}, N. Bartosik^a, R. Bellan^{a,b}, C. Biino^a, N. Cartiglia^a, F. Cenna^{a,b}, M. Costa^{a,b}, R. Covarelli^{a,b}, A. Degano^{a,b}, N. Demaria^a, B. Kiani^{a,b}, C. Mariotti^a, S. Maselli^a, E. Migliore^{a,b}, V. Monaco^{a,b}, E. Monteil^{a,b}, M. Monteno^a, M.M. Obertino^{a,b}, L. Pacher^{a,b}, N. Pastrone^a, M. Pelliccioni^a, G.L. Pinna Angioni^{a,b}, F. Ravera^{a,b}

A. Romero^{a,b}, M. Ruspa^{a,c}, R. Sacchi^{a,b}, K. Shchelina^{a,b}, V. Sola^a, A. Solano^{a,b}, A. Staiano^a, P. Traczyk^{a,b}

INFN Sezione di Trieste ^a, Università di Trieste ^b, Trieste, Italy

S. Belforte^a, M. Casarsa^a, F. Cossutti^a, G. Della Ricca^{a,b}, A. Zanetti^a

Kyungpook National University, Daegu, Korea

D.H. Kim, G.N. Kim, M.S. Kim, J. Lee, S. Lee, S.W. Lee, Y.D. Oh, S. Sekmen, D.C. Son, Y.C. Yang

Chonbuk National University, Jeonju, Korea

A. Lee

Chonnam National University, Institute for Universe and Elementary Particles, Kwangju, Korea

H. Kim, D.H. Moon

Hanyang University, Seoul, Korea

J.A. Brochero Cifuentes, J. Goh, T.J. Kim

Korea University, Seoul, Korea

S. Cho, S. Choi, Y. Go, D. Gyun, S. Ha, B. Hong, Y. Jo, Y. Kim, K. Lee, K.S. Lee, S. Lee, J. Lim, S.K. Park, Y. Roh

Seoul National University, Seoul, Korea

J. Almond, J. Kim, H. Lee, S.B. Oh, B.C. Radburn-Smith, S.h. Seo, U.K. Yang, H.D. Yoo, G.B. Yu

University of Seoul, Seoul, Korea

M. Choi, H. Kim, J.H. Kim, J.S.H. Lee, I.C. Park, G. Ryu

Sungkyunkwan University, Suwon, Korea

Y. Choi, C. Hwang, J. Lee, I. Yu

Vilnius University, Vilnius, Lithuania

V. Dudenas, A. Juodagalvis, J. Vaitkus

National Centre for Particle Physics, Universiti Malaya, Kuala Lumpur, Malaysia

I. Ahmed, Z.A. Ibrahim, M.A.B. Md Ali³², F. Mohamad Idris³³, W.A.T. Wan Abdullah, M.N. Yusli, Z. Zolkapli

Centro de Investigacion y de Estudios Avanzados del IPN, Mexico City, Mexico

H. Castilla-Valdez, E. De La Cruz-Burelo, I. Heredia-De La Cruz³⁴, R. Lopez-Fernandez, J. Mejia Guisao, A. Sanchez-Hernandez

Universidad Iberoamericana, Mexico City, Mexico

S. Carrillo Moreno, C. Oropeza Barrera, F. Vazquez Valencia

Benemerita Universidad Autonoma de Puebla, Puebla, Mexico

I. Pedraza, H.A. Salazar Ibarguen, C. Uribe Estrada

Universidad Autónoma de San Luis Potosí, San Luis Potosí, Mexico

A. Morelos Pineda

University of Auckland, Auckland, New Zealand

D. Krofcheck

University of Canterbury, Christchurch, New Zealand

P.H. Butler

National Centre for Physics, Quaid-I-Azam University, Islamabad, Pakistan

A. Ahmad, M. Ahmad, Q. Hassan, H.R. Hoorani, A. Saddique, M.A. Shah, M. Shoaib, M. Waqas

National Centre for Nuclear Research, Swierk, Poland

H. Bialkowska, M. Bluj, B. Boimska, T. Frueboes, M. Górski, M. Kazana, K. Nawrocki, K. Romanowska-Rybinska, M. Szleper, P. Zalewski

Institute of Experimental Physics, Faculty of Physics, University of Warsaw, Warsaw, Poland

K. Bunkowski, A. Byszuk³⁵, K. Doroba, A. Kalinowski, M. Konecki, J. Krolikowski, M. Misiura, M. Olszewski, A. Pyskir, M. Walczak

Laboratório de Instrumentação e Física Experimental de Partículas, Lisboa, Portugal

P. Bargassa, C. Beirão Da Cruz E Silva, B. Calpas, A. Di Francesco, P. Faccioli, M. Gallinaro, J. Hollar, N. Leonardo, L. Lloret Iglesias, M.V. Nemallapudi, J. Seixas, O. Toldaiev, D. Vadrucchio, J. Varela

Joint Institute for Nuclear Research, Dubna, Russia

S. Afanasiev, P. Bunin, M. Gavrilenko, I. Golutvin, I. Gorbunov, A. Kamenev, V. Karjavin, A. Lanev, A. Malakhov, V. Matveev^{36,37}, V. Palichik, V. Perelygin, S. Shmatov, S. Shulha, N. Skatchkov, V. Smirnov, N. Voytishin, A. Zarubin

Petersburg Nuclear Physics Institute, Gatchina (St. Petersburg), Russia

Y. Ivanov, V. Kim³⁸, E. Kuznetsova³⁹, P. Levchenko, V. Murzin, V. Oreshkin, I. Smirnov, V. Sulimov, L. Uvarov, S. Vavilov, A. Vorobyev

Institute for Nuclear Research, Moscow, Russia

Yu. Andreev, A. Dermenev, S. Gninenko, N. Golubev, A. Karneyeu, M. Kirsanov, N. Krasnikov, A. Pashenkov, D. Tlisov, A. Toropin

Institute for Theoretical and Experimental Physics, Moscow, Russia

V. Epshteyn, V. Gavrillov, N. Lychkovskaya, V. Popov, I. Pozdnyakov, G. Safronov, A. Spiridonov, M. Toms, E. Vlasov, A. Zhokin

Moscow Institute of Physics and Technology, Moscow, Russia

T. Aushev, A. Bylinkin³⁷

National Research Nuclear University 'Moscow Engineering Physics Institute' (MEPhI), Moscow, Russia

M. Chadeeva⁴⁰, E. Popova, E. Tarkovskii

P.N. Lebedev Physical Institute, Moscow, Russia

V. Andreev, M. Azarkin³⁷, I. Dremin³⁷, M. Kirakosyan, A. Terkulov

Skobeltsyn Institute of Nuclear Physics, Lomonosov Moscow State University, Moscow, Russia

A. Baskakov, A. Belyaev, E. Boos, V. Bunichev, M. Dubinin⁴¹, L. Dudko, A. Ershov, A. Gribushin, V. Klyukhin, O. Kodolova, I. Lokhtin, I. Miagkov, S. Obraztsov, M. Perfilov, V. Savrin

Novosibirsk State University (NSU), Novosibirsk, Russia

V. Blinov⁴², Y. Skovpen⁴², D. Shtol⁴²

State Research Center of Russian Federation, Institute for High Energy Physics, Protvino, Russia

I. Azhgirey, I. Bayshev, S. Bitioukov, D. Elumakhov, V. Kachanov, A. Kalinin, D. Konstantinov, V. Krychkin, V. Petrov, R. Ryutin, A. Sobol, S. Troshin, N. Tyurin, A. Uzunian, A. Volkov

University of Belgrade, Faculty of Physics and Vinca Institute of Nuclear Sciences, Belgrade, Serbia

P. Adzic⁴³, P. Cirkovic, D. Devetak, M. Dordevic, J. Milosevic, V. Rekovic

Centro de Investigaciones Energéticas Medioambientales y Tecnológicas (CIEMAT), Madrid, Spain

J. Alcaraz Maestre, M. Barrio Luna, M. Cerrada, N. Colino, B. De La Cruz, A. Delgado Peris, A. Escalante Del Valle, C. Fernandez Bedoya, J.P. Fernández Ramos, J. Flix, M.C. Fouz, P. Garcia-Abia, O. Gonzalez Lopez, S. Goy Lopez, J.M. Hernandez, M.I. Josa, A. Pérez-Calero Yzquierdo, J. Puerta Pelayo, A. Quintario Olmeda, I. Redondo, L. Romero, M.S. Soares

Universidad Autónoma de Madrid, Madrid, Spain

J.F. de Trocóniz, M. Missiroli, D. Moran

Universidad de Oviedo, Oviedo, Spain

J. Cuevas, C. Erice, J. Fernandez Menendez, I. Gonzalez Caballero, J.R. González Fernández, E. Palencia Cortezon, S. Sanchez Cruz, I. Suárez Andrés, P. Vischia, J.M. Vizan Garcia

Instituto de Física de Cantabria (IFCA), CSIC-Universidad de Cantabria, Santander, Spain

I.J. Cabrillo, A. Calderon, B. Chazin Quero, E. Curras, M. Fernandez, J. Garcia-Ferrero, G. Gomez, A. Lopez Virto, J. Marco, C. Martinez Rivero, F. Matorras, J. Piedra Gomez, T. Rodrigo, A. Ruiz-Jimeno, L. Scodellaro, N. Trevisani, I. Vila, R. Vilar Cortabitarte

CERN, European Organization for Nuclear Research, Geneva, Switzerland

D. Abbaneo, E. Auffray, P. Baillon, A.H. Ball, D. Barney, M. Bianco, P. Bloch, A. Bocci, C. Botta, T. Camporesi, R. Castello, M. Cepeda, G. Cerminara, Y. Chen, D. d'Enterria, A. Dabrowski, V. Daponte, A. David, M. De Gruttola, A. De Roeck, E. Di Marco⁴⁴, M. Dobson, B. Dorney, T. du Pree, M. Dünser, N. Dupont, A. Elliott-Peisert, P. Everaerts, G. Franzoni, J. Fulcher, W. Funk, D. Gigi, K. Gill, F. Glege, D. Gulhan, S. Gundacker, M. Guthoff, P. Harris, J. Hegeman, V. Innocente, P. Janot, O. Karacheban¹⁸, J. Kieseler, H. Kirschenmann, V. Knünz, A. Kornmayer¹⁵, M.J. Kortelainen, C. Lange, P. Lecoq, C. Lourenço, M.T. Lucchini, L. Malgeri, M. Mannelli, A. Martelli, F. Meijers, J.A. Merlin, S. Mersi, E. Meschi, P. Milenovic⁴⁵, F. Moortgat, M. Mulders, H. Neugebauer, S. Orfanelli, L. Orsini, L. Pape, E. Perez, M. Peruzzi, A. Petrilli, G. Petrucciani, A. Pfeiffer, M. Pierini, A. Racz, T. Reis, G. Rolandi⁴⁶, M. Rovere, H. Sakulin, J.B. Sauvan, C. Schäfer, C. Schwick, M. Seidel, A. Sharma, P. Silva, P. Sphicas⁴⁷, J. Steggemann, M. Stoye, M. Tosi, D. Treille, A. Triossi, A. Tsirou, V. Veckalns⁴⁸, G.I. Veres²⁰, M. Verweij, N. Wardle, W.D. Zeuner

Paul Scherrer Institut, Villigen, Switzerland

W. Bertl, K. Deiters, W. Erdmann, R. Horisberger, Q. Ingram, H.C. Kaestli, D. Kotlinski, U. Langenegger, T. Rohe, S.A. Wiederkehr

Institute for Particle Physics, ETH Zurich, Zurich, Switzerland

F. Bachmair, L. Bäni, P. Berger, L. Bianchini, B. Casal, G. Dissertori, M. Dittmar, M. Donegà, C. Grab, C. Heidegger, D. Hits, J. Hoss, G. Kasieczka, T. Klijnsma, W. Lustermann, B. Mangano, M. Marionneau, P. Martinez Ruiz del Arbol, M. Masciovecchio, M.T. Meinhard, D. Meister, F. Micheli, P. Musella, F. Nessi-Tedaldi, F. Pandolfi, J. Pata, F. Pauss, G. Perrin, L. Perrozzi, M. Quittnat, M. Rossini, M. Schönenberger, L. Shchutska, A. Starodumov⁴⁹, V.R. Tavolaro, K. Theofilatos, M.L. Vesterbacka Olsson, R. Wallny, A. Zagozdinska³⁵, D.H. Zhu

Universität Zürich, Zurich, Switzerland

T.K. Aarrestad, C. AMSler⁵⁰, L. Caminada, M.F. Canelli, A. De Cosa, S. Donato, C. Galloni,

A. Hinzmann, T. Hreus, B. Kilminster, J. Ngadiuba, D. Pinna, G. Rauco, P. Robmann, D. Salerno, C. Seitz, Y. Yang, A. Zucchetta

National Central University, Chung-Li, Taiwan

V. Candelise, T.H. Doan, Sh. Jain, R. Khurana, M. Konyushikhin, C.M. Kuo, W. Lin, A. Pozdnyakov, S.S. Yu

National Taiwan University (NTU), Taipei, Taiwan

Arun Kumar, P. Chang, Y.H. Chang, Y. Chao, K.F. Chen, P.H. Chen, F. Fiori, W.-S. Hou, Y. Hsiung, Y.F. Liu, R.-S. Lu, M. Miñano Moya, E. Paganis, A. Psallidas, J.f. Tsai

Chulalongkorn University, Faculty of Science, Department of Physics, Bangkok, Thailand

B. Asavapibhop, K. Kovitanggoon, G. Singh, N. Srimanobhas

Cukurova University, Physics Department, Science and Art Faculty, Adana, Turkey

A. Adiguzel⁵¹, F. Boran, S. Cerci⁵², S. Damarseckin, Z.S. Demiroglu, C. Dozen, I. Dumanoglu, S. Girgis, G. Gokbulut, Y. Guler, I. Hos⁵³, E.E. Kangal⁵⁴, O. Kara, U. Kiminsu, M. Oglakci, G. Onengut⁵⁵, K. Ozdemir⁵⁶, D. Sunar Cerci⁵², B. Tali⁵², H. Topakli⁵⁷, S. Turkcapar, I.S. Zorbakir, C. Zorbilmez

Middle East Technical University, Physics Department, Ankara, Turkey

B. Bilin, G. Karapinar⁵⁸, K. Ocalan⁵⁹, M. Yalvac, M. Zeyrek

Bogazici University, Istanbul, Turkey

E. Gülmez, M. Kaya⁶⁰, O. Kaya⁶¹, E.A. Yetkin⁶²

Istanbul Technical University, Istanbul, Turkey

A. Cakir, K. Cankocak

Institute for Scintillation Materials of National Academy of Science of Ukraine, Kharkov, Ukraine

B. Grynyov

National Scientific Center, Kharkov Institute of Physics and Technology, Kharkov, Ukraine

L. Levchuk, P. Sorokin

University of Bristol, Bristol, United Kingdom

R. Aggleton, F. Ball, L. Beck, J.J. Brooke, D. Burns, E. Clement, D. Cussans, H. Flacher, J. Goldstein, M. Grimes, G.P. Heath, H.F. Heath, J. Jacob, L. Kreczko, C. Lucas, D.M. Newbold⁶³, S. Paramesvaran, A. Poll, T. Sakuma, S. Seif El Nasr-storey, D. Smith, V.J. Smith

Rutherford Appleton Laboratory, Didcot, United Kingdom

K.W. Bell, A. Belyaev⁶⁴, C. Brew, R.M. Brown, L. Calligaris, D. Cieri, D.J.A. Cockerill, J.A. Coughlan, K. Harder, S. Harper, E. Olaiya, D. Petyt, C.H. Shepherd-Themistocleous, A. Thea, I.R. Tomalin, T. Williams

Imperial College, London, United Kingdom

M. Baber, R. Bainbridge, O. Buchmuller, A. Bundock, S. Casasso, M. Citron, D. Colling, L. Corpe, P. Dauncey, G. Davies, A. De Wit, M. Della Negra, R. Di Maria, P. Dunne, A. Elwood, D. Futyan, Y. Haddad, G. Hall, G. Iles, T. James, R. Lane, C. Laner, L. Lyons, A.-M. Magnan, S. Malik, L. Mastrolorenzo, J. Nash, A. Nikitenko⁴⁹, J. Pela, M. Pesaresi, D.M. Raymond, A. Richards, A. Rose, E. Scott, C. Seez, S. Summers, A. Tapper, K. Uchida, M. Vazquez Acosta⁶⁵, T. Virdee¹⁵, J. Wright, S.C. Zenz

Brunel University, Uxbridge, United Kingdom

J.E. Cole, P.R. Hobson, A. Khan, P. Kyberd, I.D. Reid, P. Symonds, L. Teodorescu, M. Turner

Baylor University, Waco, USA

A. Borzou, K. Call, J. Dittmann, K. Hatakeyama, H. Liu, N. Pastika

Catholic University of America, Washington, USA

R. Bartek, A. Dominguez

The University of Alabama, Tuscaloosa, USA

A. Buccilli, S.I. Cooper, C. Henderson, P. Rumerio, C. West

Boston University, Boston, USA

D. Arcaro, A. Avetisyan, T. Bose, D. Gastler, D. Rankin, C. Richardson, J. Rohlf, L. Sulak, D. Zou

Brown University, Providence, USA

G. Benelli, D. Cutts, A. Garabedian, J. Hakala, U. Heintz, J.M. Hogan, K.H.M. Kwok, E. Laird, G. Landsberg, Z. Mao, M. Narain, S. Piperov, S. Sagir, R. Syarif

University of California, Davis, Davis, USA

R. Band, C. Brainerd, D. Burns, M. Calderon De La Barca Sanchez, M. Chertok, J. Conway, R. Conway, P.T. Cox, R. Erbacher, C. Flores, G. Funk, M. Gardner, W. Ko, R. Lander, C. Mclean, M. Mulhearn, D. Pellett, J. Pilot, S. Shalhout, M. Shi, J. Smith, M. Squires, D. Stolp, K. Tos, M. Tripathi, Z. Wang

University of California, Los Angeles, USA

M. Bachtis, C. Bravo, R. Cousins, A. Dasgupta, A. Florent, J. Hauser, M. Ignatenko, N. Mccoll, D. Saltzberg, C. Schnaible, V. Valuev

University of California, Riverside, Riverside, USA

E. Bouvier, K. Burt, R. Clare, J. Ellison, J.W. Gary, S.M.A. Ghiasi Shirazi, G. Hanson, J. Heilman, P. Jandir, E. Kennedy, F. Lacroix, O.R. Long, M. Olmedo Negrete, M.I. Paneva, A. Shrinivas, W. Si, H. Wei, S. Wimpenny, B. R. Yates

University of California, San Diego, La Jolla, USA

J.G. Branson, G.B. Cerati, S. Cittolin, M. Derdzinski, A. Holzner, D. Klein, G. Kole, V. Krutelyov, J. Letts, I. Macneill, D. Olivito, S. Padhi, M. Pieri, M. Sani, V. Sharma, S. Simon, M. Tadel, A. Vartak, S. Wasserbaech⁶⁶, F. Würthwein, A. Yagil, G. Zevi Della Porta

University of California, Santa Barbara - Department of Physics, Santa Barbara, USA

N. Amin, R. Bhandari, J. Bradmiller-Feld, C. Campagnari, A. Dishaw, V. Dutta, M. Franco Sevilla, C. George, F. Golf, L. Gouskos, J. Gran, R. Heller, J. Incandela, S.D. Mullin, A. Ovcharova, H. Qu, J. Richman, D. Stuart, I. Suarez, J. Yoo

California Institute of Technology, Pasadena, USA

D. Anderson, J. Bendavid, A. Bornheim, J.M. Lawhorn, H.B. Newman, T. Nguyen, C. Pena, M. Spiropulu, J.R. Vlimant, S. Xie, Z. Zhang, R.Y. Zhu

Carnegie Mellon University, Pittsburgh, USA

M.B. Andrews, T. Ferguson, M. Paulini, J. Russ, M. Sun, H. Vogel, I. Vorobiev, M. Weinberg

University of Colorado Boulder, Boulder, USA

J.P. Cumalat, W.T. Ford, F. Jensen, A. Johnson, M. Krohn, S. Leontsinis, T. Mulholland, K. Stenson, S.R. Wagner

Cornell University, Ithaca, USA

J. Alexander, J. Chaves, J. Chu, S. Dittmer, K. Mcdermott, N. Mirman, J.R. Patterson, A. Rinkevicius, A. Ryd, L. Skinnari, L. Soffi, S.M. Tan, Z. Tao, J. Thom, J. Tucker, P. Wittich, M. Zientek

Fairfield University, Fairfield, USA

D. Winn

Fermi National Accelerator Laboratory, Batavia, USA

S. Abdullin, M. Albrow, G. Apollinari, A. Apresyan, A. Apyan, S. Banerjee, L.A.T. Bauerdick, A. Beretvas, J. Berryhill, P.C. Bhat, G. Bolla, K. Burkett, J.N. Butler, A. Canepa, H.W.K. Cheung, F. Chlebana, M. Cremonesi, J. Duarte, V.D. Elvira, I. Fisk, J. Freeman, Z. Gecse, E. Gottschalk, L. Gray, D. Green, S. Grünendahl, O. Gutsche, R.M. Harris, S. Hasegawa, J. Hirschauer, Z. Hu, B. Jayatilaka, S. Jindariani, M. Johnson, U. Joshi, B. Klima, B. Kreis, S. Lammel, D. Lincoln, R. Lipton, M. Liu, T. Liu, R. Lopes De Sá, J. Lykken, K. Maeshima, N. Magini, J.M. Marraffino, S. Maruyama, D. Mason, P. McBride, P. Merkel, S. Mrenna, S. Nahn, V. O'Dell, K. Pedro, O. Prokofyev, G. Rakness, L. Ristori, B. Schneider, E. Sexton-Kennedy, A. Soha, W.J. Spalding, L. Spiegel, S. Stoynev, J. Strait, N. Strobbe, L. Taylor, S. Tkaczyk, N.V. Tran, L. Uplegger, E.W. Vaandering, C. Vernieri, M. Verzocchi, R. Vidal, M. Wang, H.A. Weber, A. Whitbeck

University of Florida, Gainesville, USA

D. Acosta, P. Avery, P. Bortignon, A. Brinkerhoff, A. Carnes, M. Carver, D. Curry, S. Das, R.D. Field, I.K. Furic, J. Konigsberg, A. Korytov, K. Kotov, P. Ma, K. Matchev, H. Mei, G. Mitselmakher, D. Rank, D. Sperka, N. Terentyev, L. Thomas, J. Wang, S. Wang, J. Yelton

Florida International University, Miami, USA

S. Linn, P. Markowitz, G. Martinez, J.L. Rodriguez

Florida State University, Tallahassee, USA

A. Ackert, T. Adams, A. Askew, S. Hagopian, V. Hagopian, K.F. Johnson, T. Kolberg, T. Perry, H. Prosper, A. Santra, R. Yohay

Florida Institute of Technology, Melbourne, USA

M.M. Baarmand, V. Bhopatkar, S. Colafranceschi, M. Hohmann, D. Noonan, T. Roy, F. Yumiceva

University of Illinois at Chicago (UIC), Chicago, USA

M.R. Adams, L. Apanasevich, D. Berry, R.R. Betts, R. Cavanaugh, X. Chen, O. Evdokimov, C.E. Gerber, D.A. Hangal, D.J. Hofman, K. Jung, J. Kamin, I.D. Sandoval Gonzalez, M.B. Tonjes, H. Trauger, N. Varelas, H. Wang, Z. Wu, J. Zhang

The University of Iowa, Iowa City, USA

B. Bilki⁶⁷, W. Clarida, K. Dilsiz⁶⁸, S. Durgut, R.P. Gandrajula, M. Haytmyradov, V. Khristenko, J.-P. Merlo, H. Mermerkaya⁶⁹, A. Mestvirishvili, A. Moeller, J. Nachtman, H. Ogul⁷⁰, Y. Onel, F. Ozok⁷¹, A. Penzo, C. Snyder, E. Tiras, J. Wetzel, K. Yi

Johns Hopkins University, Baltimore, USA

B. Blumenfeld, A. Cocoros, N. Eminizer, D. Fehling, L. Feng, A.V. Gritsan, P. Maksimovic, J. Roskes, U. Sarica, M. Swartz, M. Xiao, C. You

The University of Kansas, Lawrence, USA

A. Al-bataineh, P. Baringer, A. Bean, S. Boren, J. Bowen, J. Castle, S. Khalil, A. Kropivnitskaya, D. Majumder, W. Mcbrayer, M. Murray, C. Royon, S. Sanders, E. Schmitz, R. Stringer, J.D. Tapia Takaki, Q. Wang

Kansas State University, Manhattan, USA

A. Ivanov, K. Kaadze, Y. Maravin, A. Mohammadi, L.K. Saini, N. Skhirtladze, S. Toda

Lawrence Livermore National Laboratory, Livermore, USA

F. Rebassoo, D. Wright

University of Maryland, College Park, USA

C. Anelli, A. Baden, O. Baron, A. Belloni, B. Calvert, S.C. Eno, C. Ferraioli, N.J. Hadley, S. Jabeen, G.Y. Jeng, R.G. Kellogg, J. Kunkle, A.C. Mignerey, F. Ricci-Tam, Y.H. Shin, A. Skuja, S.C. Tonwar

Massachusetts Institute of Technology, Cambridge, USA

D. Abercrombie, B. Allen, V. Azzolini, R. Barbieri, A. Baty, R. Bi, S. Brandt, W. Busza, I.A. Cali, M. D'Alfonso, Z. Demiragli, G. Gomez Ceballos, M. Goncharov, D. Hsu, Y. Iiyama, G.M. Innocenti, M. Klute, D. Kovalskyi, Y.S. Lai, Y.-J. Lee, A. Levin, P.D. Luckey, B. Maier, A.C. Marini, C. Mcginn, C. Mironov, S. Narayanan, X. Niu, C. Paus, C. Roland, G. Roland, J. Salfeld-Nebgen, G.S.F. Stephans, K. Tatar, D. Velicanu, J. Wang, T.W. Wang, B. Wyslouch

University of Minnesota, Minneapolis, USA

A.C. Benvenuti, R.M. Chatterjee, A. Evans, P. Hansen, S. Kalafut, S.C. Kao, Y. Kubota, Z. Lesko, J. Mans, S. Nourbakhsh, N. Ruckstuhl, R. Rusack, N. Tambe, J. Turkewitz

University of Mississippi, Oxford, USA

J.G. Acosta, S. Oliveros

University of Nebraska-Lincoln, Lincoln, USA

E. Avdeeva, K. Bloom, D.R. Claes, C. Fangmeier, R. Gonzalez Suarez, R. Kamalieddin, I. Kravchenko, J. Monroy, J.E. Siado, G.R. Snow, B. Stieger

State University of New York at Buffalo, Buffalo, USA

M. Alyari, J. Dolen, A. Godshalk, C. Harrington, I. Iashvili, A. Kharchilava, A. Parker, S. Rappoccio, B. Roozbahani

Northeastern University, Boston, USA

G. Alverson, E. Barberis, A. Hortiangtham, A. Massironi, D.M. Morse, D. Nash, T. Orimoto, R. Teixeira De Lima, D. Trocino, R.-J. Wang, D. Wood

Northwestern University, Evanston, USA

S. Bhattacharya, O. Charaf, K.A. Hahn, N. Mucia, N. Odell, B. Pollack, M.H. Schmitt, K. Sung, M. Trovato, M. Velasco

University of Notre Dame, Notre Dame, USA

N. Dev, M. Hildreth, K. Hurtado Anampa, C. Jessop, D.J. Karmgard, N. Kellams, K. Lannon, N. Loukas, N. Marinelli, F. Meng, C. Mueller, Y. Musienko³⁶, M. Planer, A. Reinsvold, R. Ruchti, N. Rupperecht, G. Smith, S. Taroni, M. Wayne, M. Wolf, A. Woodard

The Ohio State University, Columbus, USA

J. Alimena, L. Antonelli, B. Bylsma, L.S. Durkin, S. Flowers, B. Francis, A. Hart, C. Hill, W. Ji, B. Liu, W. Luo, D. Puigh, B.L. Winer, H.W. Wulsin

Princeton University, Princeton, USA

A. Benaglia, S. Cooperstein, O. Driga, P. Elmer, J. Hardenbrook, P. Hebda, D. Lange, J. Luo, D. Marlow, K. Mei, I. Ojalvo, J. Olsen, C. Palmer, P. Piroué, D. Stickland, A. Svyatkovskiy, C. Tully

University of Puerto Rico, Mayaguez, USA

S. Malik, S. Norberg

Purdue University, West Lafayette, USA

A. Barker, V.E. Barnes, S. Folgueras, L. Gutay, M.K. Jha, M. Jones, A.W. Jung, A. Khatiwada, D.H. Miller, N. Neumeister, J.F. Schulte, J. Sun, F. Wang, W. Xie

Purdue University Northwest, Hammond, USA

T. Cheng, N. Parashar, J. Stupak

Rice University, Houston, USA

A. Adair, B. Akgun, Z. Chen, K.M. Ecklund, F.J.M. Geurts, M. Guilbaud, W. Li, B. Michlin, M. Northup, B.P. Padley, J. Roberts, J. Rorie, Z. Tu, J. Zabel

University of Rochester, Rochester, USA

B. Betchart, A. Bodek, P. de Barbaro, R. Demina, Y.t. Duh, T. Ferbel, M. Galanti, A. Garcia-Bellido, J. Han, O. Hindrichs, A. Khukhunaishvili, K.H. Lo, P. Tan, M. Verzetti

The Rockefeller University, New York, USA

R. Ciesielski, K. Goulianos, C. Mesropian

Rutgers, The State University of New Jersey, Piscataway, USA

A. Agapitos, J.P. Chou, Y. Gershtein, T.A. Gómez Espinosa, E. Halkiadakis, M. Heindl, E. Hughes, S. Kaplan, R. Kunnawalkam Elayavalli, S. Kyriacou, A. Lath, R. Montalvo, K. Nash, M. Osherson, H. Saka, S. Salur, S. Schnetzer, D. Sheffield, S. Somalwar, R. Stone, S. Thomas, P. Thomassen, M. Walker

University of Tennessee, Knoxville, USA

M. Foerster, J. Heideman, G. Riley, K. Rose, S. Spanier, K. Thapa

Texas A&M University, College Station, USA

O. Bouhali⁷², A. Castaneda Hernandez⁷², A. Celik, M. Dalchenko, M. De Mattia, A. Delgado, S. Dildick, R. Eusebi, J. Gilmore, T. Huang, T. Kamon⁷³, R. Mueller, Y. Pakhotin, R. Patel, A. Perloff, L. Perniè, D. Rathjens, A. Safonov, A. Tatarinov, K.A. Ulmer

Texas Tech University, Lubbock, USA

N. Akchurin, J. Damgov, F. De Guio, C. Dragoiu, P.R. Duderod, J. Faulkner, E. Gurpinar, S. Kunori, K. Lamichhane, S.W. Lee, T. Libeiro, T. Peltola, S. Undleeb, I. Volobouev, Z. Wang

Vanderbilt University, Nashville, USA

S. Greene, A. Gurrola, R. Janjam, W. Johns, C. Maguire, A. Melo, H. Ni, P. Sheldon, S. Tuo, J. Velkovska, Q. Xu

University of Virginia, Charlottesville, USA

M.W. Arenton, P. Barria, B. Cox, R. Hirosky, A. Ledovskoy, H. Li, C. Neu, T. Sinthuprasith, X. Sun, Y. Wang, E. Wolfe, F. Xia

Wayne State University, Detroit, USA

C. Clarke, R. Harr, P.E. Karchin, J. Sturdy, S. Zaleski

University of Wisconsin - Madison, Madison, WI, USA

D.A. Belknap, J. Buchanan, C. Caillol, S. Dasu, L. Dodd, S. Duric, B. Gomber, M. Grothe, M. Herndon, A. Hervé, U. Hussain, P. Klabbers, A. Lanaro, A. Levine, K. Long, R. Loveless, G.A. Pierro, G. Polese, T. Ruggles, A. Savin, N. Smith, W.H. Smith, D. Taylor, N. Woods

1: Also at Vienna University of Technology, Vienna, Austria

2: Also at State Key Laboratory of Nuclear Physics and Technology, Peking University, Beijing, China

3: Also at Universidade Estadual de Campinas, Campinas, Brazil

4: Also at Universidade Federal de Pelotas, Pelotas, Brazil

5: Also at Université Libre de Bruxelles, Bruxelles, Belgium

6: Also at Joint Institute for Nuclear Research, Dubna, Russia

- 7: Also at Helwan University, Cairo, Egypt
- 8: Now at Zewail City of Science and Technology, Zewail, Egypt
- 9: Now at Fayoum University, El-Fayoum, Egypt
- 10: Also at British University in Egypt, Cairo, Egypt
- 11: Now at Ain Shams University, Cairo, Egypt
- 12: Also at Université de Haute Alsace, Mulhouse, France
- 13: Also at Skobeltsyn Institute of Nuclear Physics, Lomonosov Moscow State University, Moscow, Russia
- 14: Also at Tbilisi State University, Tbilisi, Georgia
- 15: Also at CERN, European Organization for Nuclear Research, Geneva, Switzerland
- 16: Also at RWTH Aachen University, III. Physikalisches Institut A, Aachen, Germany
- 17: Also at University of Hamburg, Hamburg, Germany
- 18: Also at Brandenburg University of Technology, Cottbus, Germany
- 19: Also at Institute of Nuclear Research ATOMKI, Debrecen, Hungary
- 20: Also at MTA-ELTE Lendület CMS Particle and Nuclear Physics Group, Eötvös Loránd University, Budapest, Hungary
- 21: Also at Institute of Physics, University of Debrecen, Debrecen, Hungary
- 22: Also at Indian Institute of Technology Bhubaneswar, Bhubaneswar, India
- 23: Also at Institute of Physics, Bhubaneswar, India
- 24: Also at University of Visva-Bharati, Santiniketan, India
- 25: Also at University of Ruhuna, Matara, Sri Lanka
- 26: Also at Isfahan University of Technology, Isfahan, Iran
- 27: Also at Yazd University, Yazd, Iran
- 28: Also at Plasma Physics Research Center, Science and Research Branch, Islamic Azad University, Tehran, Iran
- 29: Also at Università degli Studi di Siena, Siena, Italy
- 30: Also at INFN Sezione di Milano-Bicocca; Università di Milano-Bicocca, Milano, Italy
- 31: Also at Purdue University, West Lafayette, USA
- 32: Also at International Islamic University of Malaysia, Kuala Lumpur, Malaysia
- 33: Also at Malaysian Nuclear Agency, MOSTI, Kajang, Malaysia
- 34: Also at Consejo Nacional de Ciencia y Tecnología, Mexico city, Mexico
- 35: Also at Warsaw University of Technology, Institute of Electronic Systems, Warsaw, Poland
- 36: Also at Institute for Nuclear Research, Moscow, Russia
- 37: Now at National Research Nuclear University 'Moscow Engineering Physics Institute' (MEPhI), Moscow, Russia
- 38: Also at St. Petersburg State Polytechnical University, St. Petersburg, Russia
- 39: Also at University of Florida, Gainesville, USA
- 40: Also at P.N. Lebedev Physical Institute, Moscow, Russia
- 41: Also at California Institute of Technology, Pasadena, USA
- 42: Also at Budker Institute of Nuclear Physics, Novosibirsk, Russia
- 43: Also at Faculty of Physics, University of Belgrade, Belgrade, Serbia
- 44: Also at INFN Sezione di Roma; Sapienza Università di Roma, Rome, Italy
- 45: Also at University of Belgrade, Faculty of Physics and Vinca Institute of Nuclear Sciences, Belgrade, Serbia
- 46: Also at Scuola Normale e Sezione dell'INFN, Pisa, Italy
- 47: Also at National and Kapodistrian University of Athens, Athens, Greece
- 48: Also at Riga Technical University, Riga, Latvia
- 49: Also at Institute for Theoretical and Experimental Physics, Moscow, Russia
- 50: Also at Albert Einstein Center for Fundamental Physics, Bern, Switzerland

- 51: Also at Istanbul University, Faculty of Science, Istanbul, Turkey
- 52: Also at Adiyaman University, Adiyaman, Turkey
- 53: Also at Istanbul Aydin University, Istanbul, Turkey
- 54: Also at Mersin University, Mersin, Turkey
- 55: Also at Cag University, Mersin, Turkey
- 56: Also at Piri Reis University, Istanbul, Turkey
- 57: Also at Gaziosmanpasa University, Tokat, Turkey
- 58: Also at Izmir Institute of Technology, Izmir, Turkey
- 59: Also at Necmettin Erbakan University, Konya, Turkey
- 60: Also at Marmara University, Istanbul, Turkey
- 61: Also at Kafkas University, Kars, Turkey
- 62: Also at Istanbul Bilgi University, Istanbul, Turkey
- 63: Also at Rutherford Appleton Laboratory, Didcot, United Kingdom
- 64: Also at School of Physics and Astronomy, University of Southampton, Southampton, United Kingdom
- 65: Also at Instituto de Astrofísica de Canarias, La Laguna, Spain
- 66: Also at Utah Valley University, Orem, USA
- 67: Also at BEYKENT UNIVERSITY, Istanbul, Turkey
- 68: Also at Bingol University, Bingol, Turkey
- 69: Also at Erzincan University, Erzincan, Turkey
- 70: Also at Sinop University, Sinop, Turkey
- 71: Also at Mimar Sinan University, Istanbul, Istanbul, Turkey
- 72: Also at Texas A&M University at Qatar, Doha, Qatar
- 73: Also at Kyungpook National University, Daegu, Korea